Modeling of Tropical Forcing of Persistent Droughts and Pluvials over Western North America: 1856–2000*

RICHARD SEAGER, YOCHANAN KUSHNIR, CELINE HERWEIJER, NAOMI NAIK, AND JENNIFER VELEZ

Lamont-Doherty Earth Observatory, Columbia University, Palisades, New York

(Manuscript received 21 October 2004, in final form 4 March 2005)

ABSTRACT

The causes of persistent droughts and wet periods, or pluvials, over western North America are examined in model simulations of the period from 1856 to 2000. The simulations used either (i) global sea surface temperature data as a lower boundary condition or (ii) observed data in just the tropical Pacific and computed the surface ocean temperature elsewhere with a simple ocean model. With both arrangements, the model was able to simulate many aspects of the low-frequency (periods greater than 6 yr) variations of precipitation over the Great Plains and in the American Southwest including much of the nineteenth-century variability, the droughts of the 1930s (the "Dust Bowl") and 1950s, and the very wet period in the 1990s. Results indicate that the persistent droughts and pluvials were ultimately forced by persistent variations of tropical Pacific surface ocean temperatures. It is argued that ocean temperature variations outside of the tropical Pacific, but forced from the tropical Pacific, act to strengthen the droughts and pluvials. The persistent precipitation variations are part of a pattern of global variations that have a strong hemispherically and zonally symmetric component, which is akin to interannual variability, and that can be explained in terms of interactions between tropical ocean temperature variations, the subtropical jets, transient eddies, and the eddy-driven mean meridional circulation. Rossby wave propagation poleward and eastward from the tropical Pacific heating anomalies disrupts the zonal symmetry, intensifying droughts and pluvials over North America. Both mechanisms of tropical driving of extratropical precipitation variations work in summer as well as winter and can explain the year-round nature of the precipitation variations. In addition, land–atmosphere interactions over North America appear important by (i) translating winter precipitation variations into summer evaporation and, hence, precipitation anomalies and (ii) shifting the northward flow of moisture around the North Atlantic subtropical anticyclone eastward from the Plains and Southwest to the eastern seaboard and western Atlantic Ocean.

1. Introduction

Currently (September 2004) the American Southwest is enduring one of the long and severe droughts that have afflicted the region frequently since the instrumental record began in the late 1800s as well as in the more distant past. The current drought began with the demise of the 1997/98 El Niño and is in its fifth year. This is causing significant difficulties in meeting river flow and hydroelectric power generation requirements. For example, the U.S. Department of the Interior's Bureau of Reclamation reports on their Web site that for Lake Powell on the Colorado River "[i]nflow in 2002 was the lowest ever observed since the completion of Glen Canyon Dam in 1963," that in 2004 inflow "in July and August was dismal, only 35 and 29% of average" and that Lake Powell behind the dam is only 38% full (see http://www.usbr.gov/uc/water/crsp/cs_gcd.html).

The most recent drought in the American West is all the more of a shock because it comes on the heels of two decades that, according to instrumental records, were the wettest time in the Southwest in the last 150 yr with, perhaps, the exception of the "early twentieth-century North American pluvial" (Fye et al. 2003). Tree ring growth in the Southwest in these two decades was unprecedented in the last one thousand years (Swetnam and Betancourt 1998). Indeed it is tempting to follow

* Lamont-Doherty Earth Observatory Contribution Number 6792.

Corresponding author address: Dr. Richard Seager, Lamont-Doherty Earth Observatory, Palisades, NY 10964.
E-mail: rich@maatkare.ldeo.columbia.edu

Fye et al. (2003) and refer to this as the "late-twentieth-century North American pluvial." The coincidence of these two pluvials with two major developments in the history of the West is ironic: The Colorado River Compact that determined water allocations for the states of the Southwest was based on the anomalously large river flow in the first two decades of the twentieth century (Reisner 1986); the last two decades of the twentieth century were a time of huge population expansion in the desert states of the Southwest. What is the future of rainfall in the Southwest, and how will this effect the networks of water supply, irrigation, and power generation that have been developed in the region?

The Southwest is not the only region of North America to experience episodic drought. The Great Plains experienced a severe drought in the Dust Bowl years of the 1930s, so well remembered not only for the meteorological extremes of the period but also the eloquent memorialization of the devastating human cost by John Steinbeck, John Ford, Woody Guthrie, Dorothea Lange, and others. The Plains have experienced other droughts, for example, one in the years preceding and running through the Civil War. Stahle and Cleaveland (1988), based on tree ring widths, claim that this was the worst drought in Texas since 1700.

The Dust Bowl, however, stands out. It came on the heels of two decades of agricultural expansion during mostly wet conditions in which the native drought-resistant short grass prairie was replaced with drought-prone crops like wheat. When drought struck and the wheat died, horrible dust storms gripped the Plains, depositing dust as far away as Norway. Poor agricultural and economic policies transformed a natural climate perturbation into one of the worst environmental disasters of the twentieth century (Worster 1979). Drought returned in the late 1940s and 1950s. By some estimates, more land was damaged by wind erosion between 1954 and 1957 than during the mid-1930s. However, Dust Bowl conditions were averted by improved land use practices such as contour ploughing and shelter belts and because of different economic policies (Worster 1979).

Droughts also occurred before the period of European settlement, as summarized by Woodhouse and Overpeck (1998). Tree ring records, analysis of dead trees in lakes in the West, records of aeolian landscape features, and lake sediments all point to a climate regime of less precipitation in both the Plains and the Southwest prior to A.D. 1400 and going back hundreds of years (Stine 1994; Laird et al. 1996; Fritz et al. 2000; Cook et al. 2004).

Schubert et al. (2004) have shown that climate models forced by observed sea surface temperatures (SSTs) for the period from 1930 to the present can reproduce with some fidelity the history of precipitation over the Great Plains. They found that tropical SSTs were the most important, with a warm tropical Pacific Ocean leading to increased precipitation over the Plains. This is akin to interannual variability whereby the El Niño–Southern Oscillation (ENSO) affects precipitation over North America (Trenberth and Branstator 1992; Trenberth and Guillemot 1996; Mo and Higgins 1998; Seager et al. 2005).

The studies of Schubert et al. (2004) and Seager et al. (2005, hereafter S05) place Great Plains precipitation anomalies in the context of a pattern that has obvious hemispheric and zonal symmetry: when it is dry in the Plains, it is dry in the midlatitudes of each hemisphere and at almost all longitudes. It is also warm. This pattern has been explained by Seager et al. (2003a, hereafter S03) in terms of the impact that tropically forced changes in the strength and location of the subtropical jets have on the propagation of transient eddies and the eddy-driven mean meridional circulation (MMC). During La Niña events, this interaction causes eddy-driven descent in midlatitudes that suppresses precipitation.

Despite these advances in understanding precipitation variability over North America, many questions remain unanswered:

1) Droughts and pluvials over North America involve significant precipitation anomalies during the summer half year. Is this related to summertime SST variability or is a bridging mechanism needed, perhaps in the soil moisture, that carries over the impact of winter SST variability?
2) What is the relative role of tropical Pacific and global SST anomalies in driving the predictable component of Great Plains and Southwest precipitation anomalies?
3) What is the global dynamical context of droughts and pluvials over the American West?

Here we address these questions using observations and numerical climate models in an analysis of the period since 1856. Before the 1950s, upper-air data are rare and observations are largely restricted to the surface. Consequently, for a longer-term perspective, analysis of atmosphere models forced by observed SSTs are indispensable. We will use two straightforward approaches: the first forces the atmosphere model with the time history of observed SSTs everywhere, the second forces the atmosphere model only in the tropical Pacific but computes the SST anomalies elsewhere using a simple entraining mixed layer (ML) ocean model. Comparing the simulations of the two model configurations will answer most of the questions posed.

In the next section, we will describe the model arrangements. In section 3, we will analyze modeled and observed indices of precipitation in the Plains and Southwest. In section 4, we will examine the global atmosphere–ocean context of long-term precipitation variability in these two areas. In sections 5 and 6, we will examine the modeled and observed precipitation anomalies of the 1930s, 1950s, and 1990s. The zonal mean climates during these periods are discussed in section 7. Discussion and conclusions follow.

2. Model description and experimental design

a. Atmosphere model

The atmosphere general circulation model (GCM) used here is the National Center for Atmospheric Research (NCAR) Community Climate Model 3 (CCM3) described by Kiehl et al. (1998). It has triangular truncation at zonal wavenumber 42, 18 vertical levels, and a set of physical parameterizations often referred to as "state of the art." The performance of the model, including its precipitation simulation, is described in Hack et al. (1998) and Hurrell et al. (1998).

b. Ocean model

In some experiments, the atmosphere GCM is coupled to an ocean ML model, based on Russell et al. (1985), including a variable depth surface layer and a layer below that extends down to a uniform specified depth. The depth of the surface layer follows a specified seasonal cycle that is spatially variable and that follows the observed ML depth, taken to be the depth where the temperature falls more than 0.5 K cooler than the SST using the data of Levitus and Boyer (1994). The surface layer exchanges heat with the atmosphere according to the atmosphere GCMs' computation of the surface energy fluxes. The surface layer exchanges heat with the subsurface layer that is derived from the specified mass exchange and the modeled layer temperatures. The movement of heat by ocean currents in each layer is specified according to the "q-flux" formulation: a spatially varying seasonal cycle of q-flux is diagnosed for each layer as that which is required to maintain the observed climatological model temperatures when the ocean model is coupled to the atmosphere GCM (see Russell et al. 1985 for details). The q-fluxes also account for errors in the modeled surface flux (and other model errors) but, primarily, account for the ocean heat transport.

c. Model experimental design

In the Global Ocean–Global Atmosphere (GOGA) experiments, the atmosphere GCM uses observed SSTs as its lower boundary condition. These use a blend of datasets. The Hadley Centre Sea Ice and SST dataset (HadISST; Rayner et al. 2003) begins in 1870 and is global. The dataset of Kaplan et al. (1998) begins in 1856 and is not global, but does contain data in the Tropics. Therefore, for the tropical Pacific (20°N−20°S), we use Kaplan data from 1856 to 2000. From 1856 to 1870, and outside of the tropical Pacific, we use Kaplan data where available and otherwise use climatological SSTs from HadISST, smoothing in between. From 1870 on, and outside the tropical Pacific, we use the HadISST data. SSTs were smoothed linearly in latitude across a 10° wide belt between the tropical Pacific and the North and South Pacific Oceans.

For the Pacific Ocean Global Atmosphere-ML (POGA-ML) experiments, we only specify the SST in the tropical Pacific, using the Kaplan data, and compute the SSTs everywhere else using the ocean ML model. For both POGA-ML and GOGA, we generated 16 member ensembles with each member using a different initial condition on 1 January 1856. Results shown are for the ensemble mean, which (nearly) isolates the component of the climate variability forced by the imposed SSTs. This means that in the POGA-ML experiments the SST variations outside of the tropical Pacific are forced by the imposed SST variations in the tropical Pacific. They may feed back onto aspects of the global climate variability, but, even if they do, they are to be considered part of the climate response to tropical Pacific variations and not as causal agents that autonomously generate climate variability.

3. Modeled and observed indices of precipitation over the Great Plains and Southwest: 1856–2000

A straightforward test of the extent to which precipitation variability over North America is boundary forced and the ability of the climate model to simulate this is a comparison of the ensemble mean modeled and observed precipitation averaged over representative areas in each region. A low correlation could indicate that either the observed precipitation variability was caused by internal atmospheric variability or that, if it was SST forced, the model was unable to capture this. In contrast, a high correlation would be expected only if the observed precipitation variability was significantly forced by SST variations and the model was able to capture this. In reality only a portion of the real-world variability is expected to be SST forced, and the model's skill is limited. Consequently, the strength of the correlation is a measure of the ratio of forced precipitation variability to internal atmospheric variability and also of the model skill.

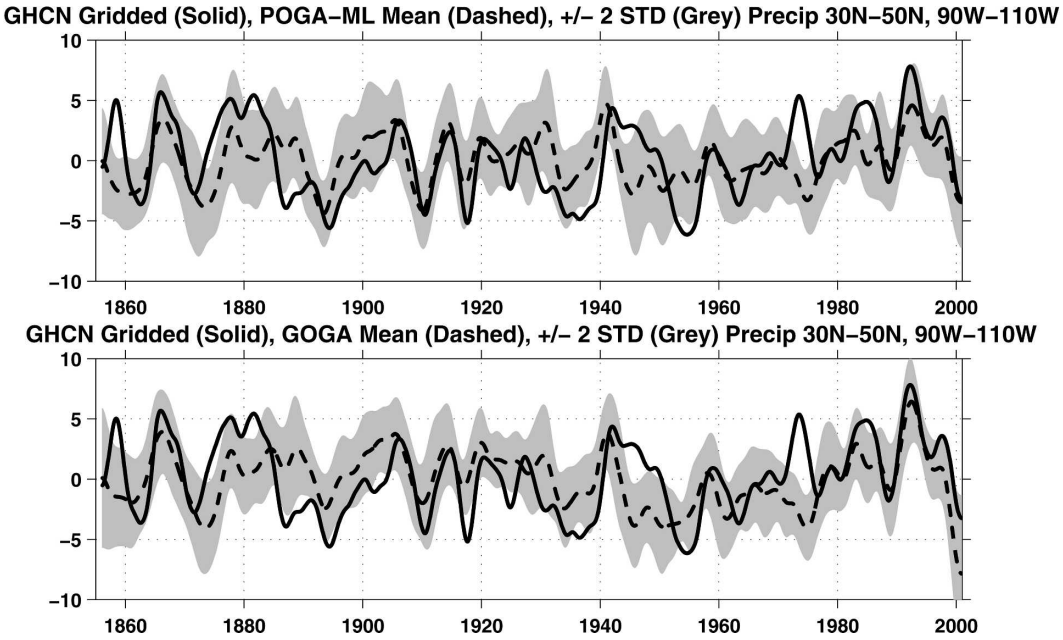

FIG. 1. (a) The precipitation anomaly (mm month^{-1}) over the Great Plains (30°–50°N, 110°–90°W) for the period 1856–2000 from the POGA-ML ensemble mean and from gridded station data. (b) Same as in (a), but with the GOGA ensemble mean. All data have been 6-yr low-pass filtered. The shading encloses the ensemble members within plus or minus of two standard deviations of the ensemble spread at any time.

For precipitation, the station data used are from the Global Historical Climate Network (GHCN) gridded by binning into boxes of four degrees of latitude and longitude. Precipitation data for almost all of North America are extremely sparse before the twentieth century with coverage gradually shifting from the east to the west, from a wetter to a drier climate, following immigrant settlement. To reduce problems associated with changing spatial coverage, precipitation anomalies were computed in each grid box before averaging these together to create spatial averages over large areas of the American West.

The indices presented here cover two areas. The first is the "Great Plains" and extends from 30° to 50°N and from 110° to 90°W, similar to the area defined by Schubert et al. (2004). The second is the "Southwest" and covers 25° to 40°N and 120° to 95°W. The observed and model data have all been subjected to a 6-yr low-pass filter to remove the effects of interannual variability and to retain variability on time scales of just under a decade and longer. All months of the year are included in the indices. Figure 1 shows results for the Great Plains. The GHCN station data are in each panel together with the POGA-ML ensemble mean in the top panel and the GOGA ensemble mean in the lower panel. The shaded area is bounded by the ensemble mean plus and minus two standard deviations of the model ensemble spread at each time. Figure 2 shows results for the Southwest in the same arrangement.

First of all, the POGA-ML and GOGA precipitation time series are very similar to each other. This makes the case that, in the model, the component of the precipitation variability that is SST forced can be obtained from SST forcing in the tropical Pacific alone. Consequently, if SST anomalies outside the tropical Pacific impact Plains or Southwest precipitation, they were themselves initially forced as a remote response to tropical Pacific variability.

The models underestimate the severity and length of the Dust Bowl drought. The models simulate a protracted dry spell beginning in the 1940s and extending through the 1950s. In reality, there was a short but severe drought in the Plains in the 1950s and a widespread drought in the West in the 1940s and 1950s. The models capture well the pluvial in the 1980s and the 1990s, the dry and wet variability between 1900 and the Dust Bowl, and much of the nineteenth-century variability.

In the Southwest, the models successfully simulate the low-frequency variability of precipitation over the last 150 yr. Individual wet spells of several years duration, such as in the 1900s, the 1910s, around the 1941/42 El Niño, and in the 1990s, are captured, albeit with frequent phase shifts of a year or so. The model also

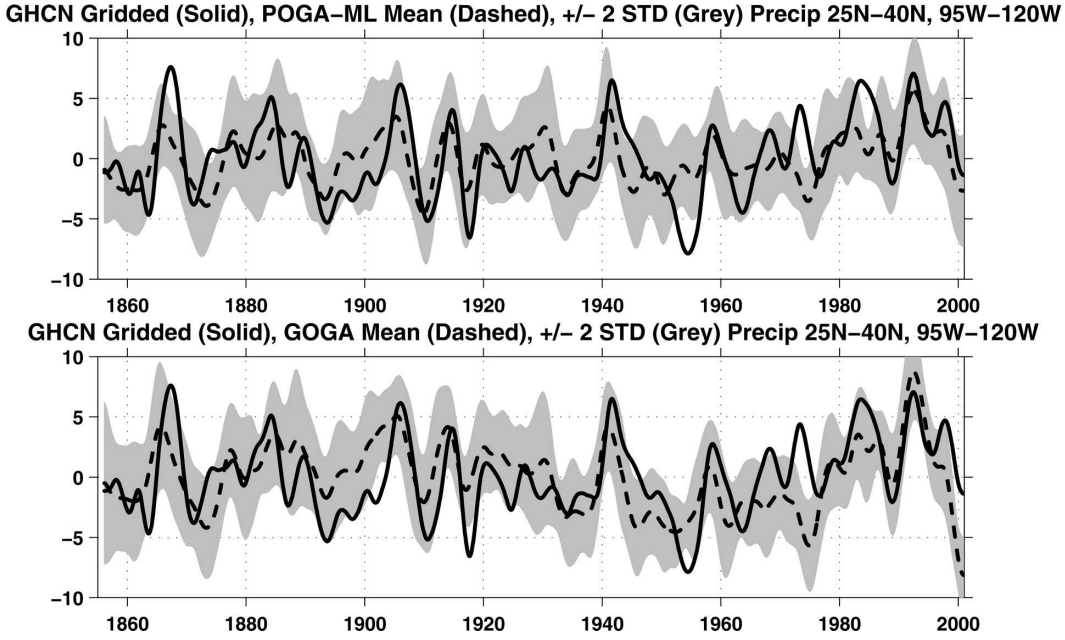

FIG. 2. Same as in Fig. 1, but for the Southwest (25°–40°N, 120°–95°W).

captures the multidecadal variability: a prolonged period that was mostly wet in the first few decades of the twentieth century, followed by a dry period between the 1940s and 1960s and ending in a very wet period in the 1980s and 1990s.

The correlation coefficient between the low-frequency variations of precipitation in the Great Plains and the Southwest is 0.83 and is higher in the model ensemble means, suggesting that on these time scales they vary together and both are SST forced. The close association between the time history of the ensemble mean low-frequency precipitation, here illustrated for the Great Plains, and the low-frequency variations of tropical SSTs is shown in Fig. 3.

Comparing a model ensemble mean, which captures only the SST-forced component, with nature, which, being a single realization, includes a substantial noise component, is troublesome. Here we are interested primarily in that part of the variability that is SST forced and, hence, potentially predictable. The correlation coefficients between the ensemble means and observed precipitation time series in Figs. 1 and 2 are just over 0.4, and it was almost as high in each of the ensemble members, suggesting that about 15%–20% of the precipitation variability is SST forced. For the 1930s and 1950s droughts and the 1990s pluvial, all, or almost all, of the GOGA ensemble members (as shown by the shading in Figs. 1 and 2) are dry or wet, respectively,

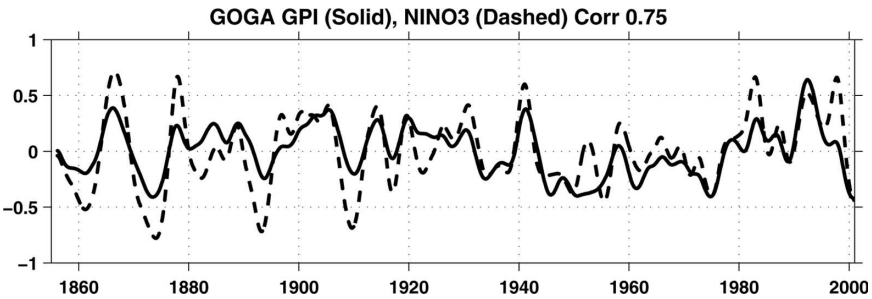

FIG. 3. The 6-yr low-passed time histories of the precipitation anomaly (cm month^{-1}) over the Great Plains (30°–50°N, 110°–90°W) for the period 1856–2000 from the GOGA ensemble mean and the observed Niño-3 SST index (SST anomalies averaged over 5°S–5°N and 150°–90°W). The correlation coefficient between the time series is 0.75.

which strengthens the argument that these events were forced by variations of SST.

Having demonstrated that the low-frequency behavior of the precipitation in the Great Plains and the Southwest was significantly forced from the tropical Pacific, we next examine the associated large-scale atmosphere and ocean variability.

4. The global atmosphere–ocean context of precipitation variability in the Great Plains and Southwest

To examine what patterns of SST variations were responsible for precipitation regimes over North America during the last century and a half, we regressed the observed SSTs on the observed precipitation indices (Figs. 1 and 2) and did the same with the modeled precipitation indices and SSTs in the model ensembles. So, as before, we are examining variability on time scales of 6 yr and longer. For the observed and the GOGA ensemble precipitation, the results show the pattern of global SST anomalies that are associated with wet conditions in these two regions in observations or the model, respectively. For the POGA-ML ensemble, it will show the pattern of tropical Pacific SST anomalies that force wet conditions in the two regions of the model *and* the pattern of SST anomalies outside of the tropical Pacific that are forced by the tropical Pacific SST variations.

Figure 4a shows the observed SST and precipitation regressions for the Great Plains. Wet conditions in the Plains are related to an El Niño–like SST anomaly pattern with a warm equatorial Pacific, warm Indian Ocean, cool waters in the central North and South Pacific, and warm waters along the coasts of the Americas. This low-frequency pattern is very similar to the interannual ENSO pattern indicating that the relationships that hold between the tropical Pacific and Plains precipitation on the year-to-year time scale [S05; Trenberth and Branstator (1992)] also hold on longer time scales, a point previously made by Schubert et al. (2004).

Figure 4b shows the SST regression from the GOGA ensemble mean. In this case the SST that goes into the regression is the same as that in Fig. 4a, but the Great Plains precipitation time series is taken from the model. The spatial pattern of SST variability is very similar to that observed in almost all details. However the regression coefficients and correlation coefficients (not shown) between Great Plains precipitation and tropical Pacific SSTs are about twice that observed. This is consistent with the model ensemble mean isolating the SST-forced component of the Great Plains precipitation, as individual ensemble members have coefficients similar to those observed.

Figure 4c shows the regression of the SSTs from the POGA-ML ensemble, which computes SSTs outside of the tropical Pacific. What is remarkable about Fig. 4c is how similar the pattern of SST anomalies is to that in the GOGA ensemble, that is, the model faithfully reproduces the SST anomalies outside of the tropical Pacific that are associated with wet conditions in the Plains. However, the modeled SST anomalies are weaker than observed, an error that might be caused by surface flux anomalies that are too weak. Nonetheless it is fair to say that, although the warm Indian Ocean, cool central and western North Pacific, and warm eastern North Pacific may have impacts on Plains precipitation, these SST anomalies are generated as remote responses to tropical Pacific SST anomalies and have limited predictive power in and of themselves.

Figure 5 shows the comparable patterns for regression on the time series of Southwest precipitation. The spatial patterns are very similar to those linking together Great Plains precipitation and global SSTs, strongly suggesting that dry and wet conditions in the Plains and the Southwest both arise from tropical forcing and are not dynamically distinct.

To identify the global patterns of precipitation and upper-tropospheric circulation associated with wet conditions in the Plains and Southwest, we focus on the POGA-ML simulations and regress global precipitation and 200-mb height on the Plains precipitation index (Fig. 6). The results can be generalized because of the similarity of both the Plains and Southwest precipitation indices and the GOGA and POGA-ML simulations. When the Plains and Southwest are wet, there is increased precipitation in the central equatorial Pacific. Wet conditions also prevail throughout the midlatitudes of both hemispheres, and the subtropics are dry. The global patterns of precipitation and atmospheric circulation that accompany low-frequency precipitation changes in North America are akin to those that accompany interannual ENSO variability.[1] Tropical upper-troposphere geopotential heights are raised, a consequence of tropical warming (Horel and Wallace 1981; Yulaeva and Wallace 1994), which is likely due, in part, to increased surface heat flux from the ocean to the atmosphere (Sun 2000), but heights are low in the midlatitudes of each hemisphere reflecting cooling during El Niño events (S03). Generally, when the midlatitudes

[1] Seager et al. (2004) show that the CCM3 model quite faithfully reproduces interannual fluctuations of the circulation forced by ENSO as well as decadal fluctuations but that the amplitude of the latter can be underestimated.

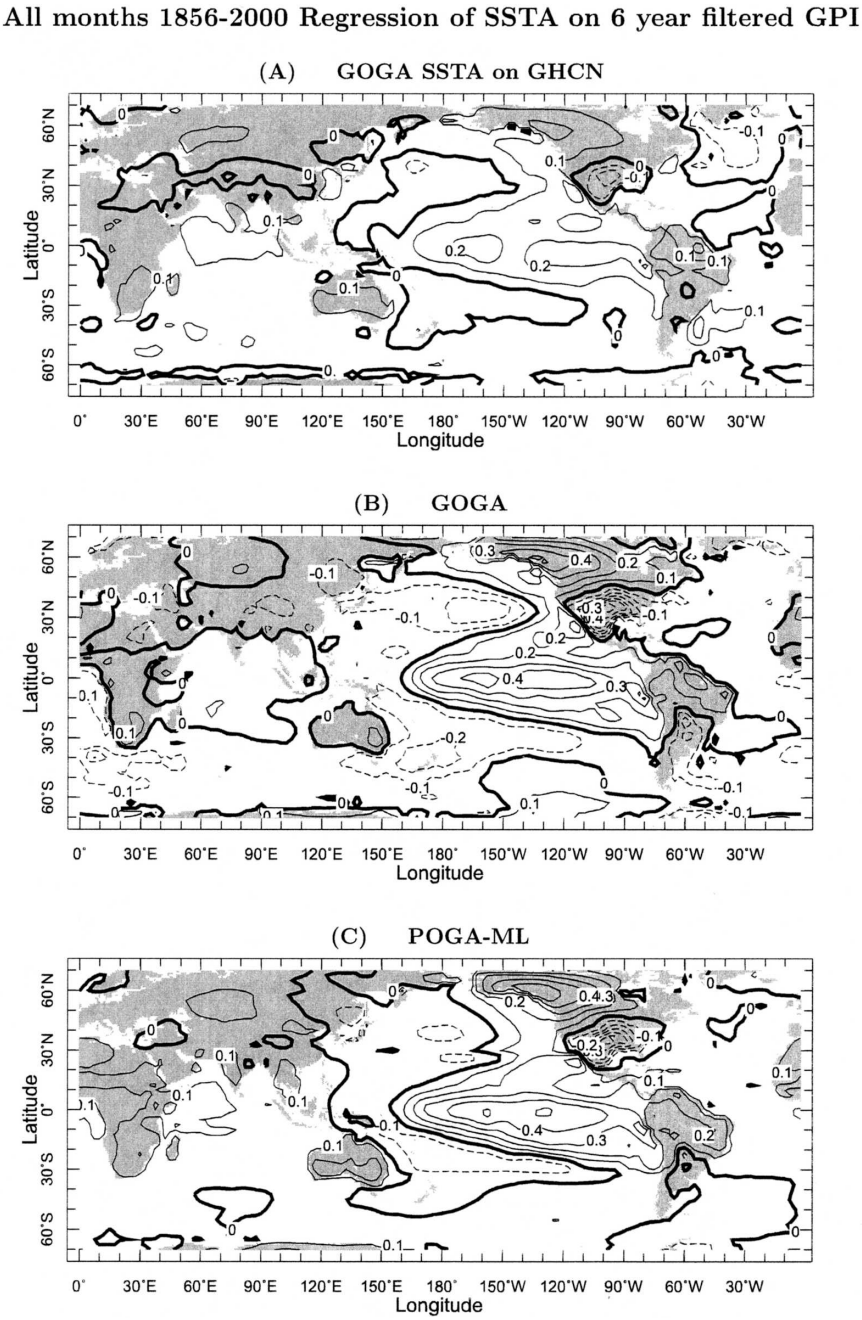

FIG. 4. Patterns of global SST regressions on time series of low-pass-filtered Great Plains precipitation for 1856–2000. (a) The observed precipitation and observed global SSTs, (b) the GOGA ensemble mean precipitation and observed global SSTs, and (c) the POGA-ML ensemble mean precipitation and the POGA-ML SSTs (observed in the tropical Pacific and computed elsewhere).

are anomalously wet, they are also cool, and vice versa. The degree of zonal symmetry in the signal helps explain the results of Hoerling and Kumar (2003), which show that the recent drought in the West went along with drought in the Mediterranean and central Asia.

To further examine the mechanisms underlying long-term changes in precipitation over North America, we next examine specific periods: the 1930s Dust Bowl drought, the late 1940s to 1950s drought over the Southwest, and the wet period in the 1990s.

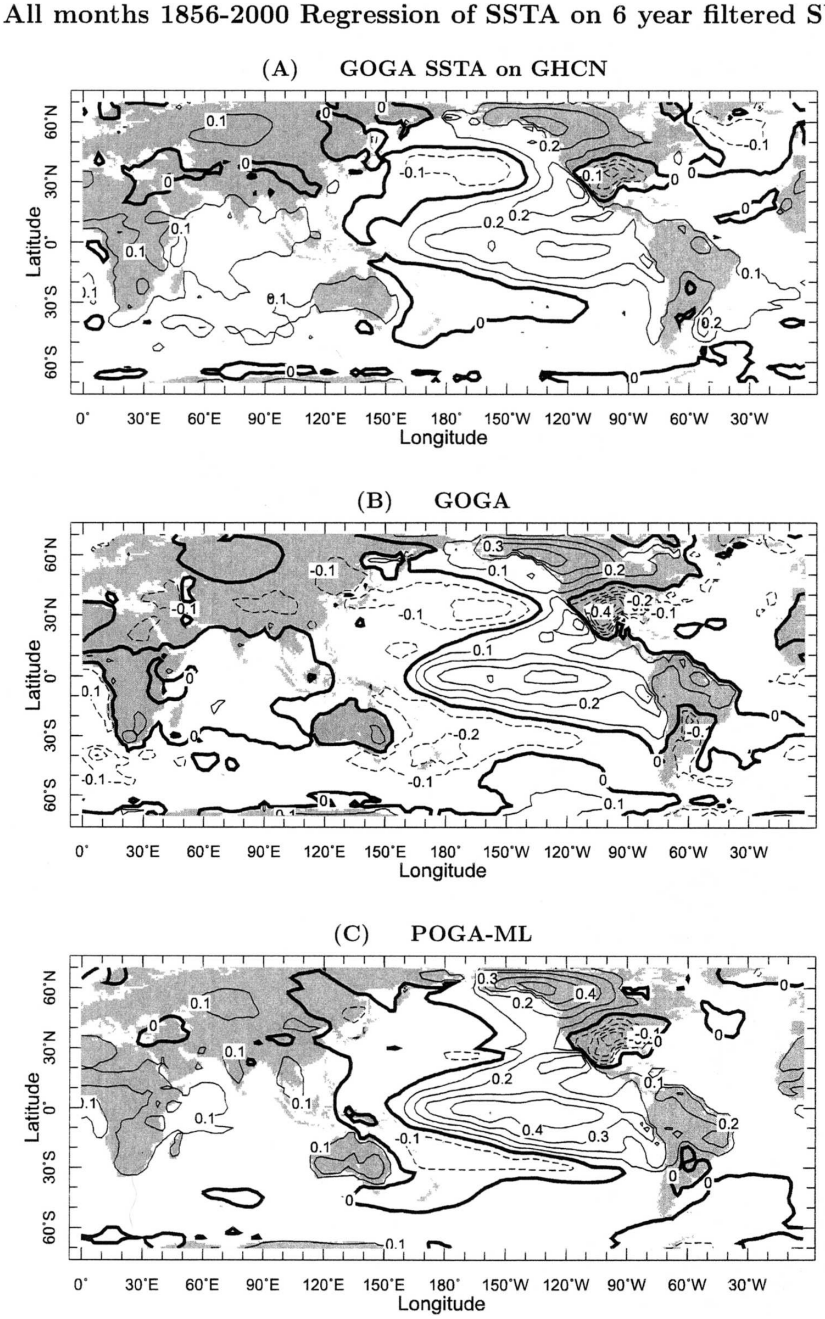

FIG. 5. Same as in Fig. 3, but for the Southwest precipitation time series.

5. Simulation of long-term droughts and pluvials in the American West during the twentieth century

In this section, we contrast modeled and observed persistent precipitation anomalies that occurred within the twentieth century. Similar events occurred during the nineteenth century, but the sparsity of precipitation data at that time means that proxy evidence, especially tree rings, must be used as verification. That exercise is beyond the scope of the current paper and will be considered in a separate manuscript (C. Herweijer et al. 2005, manuscript submitted to *Holocene*).

a. The 1930s "Dust Bowl" drought

The 1930s Dust Bowl drought was one of the most severe droughts in the Great Plains in the last two centuries, and the one with the most severe human conse-

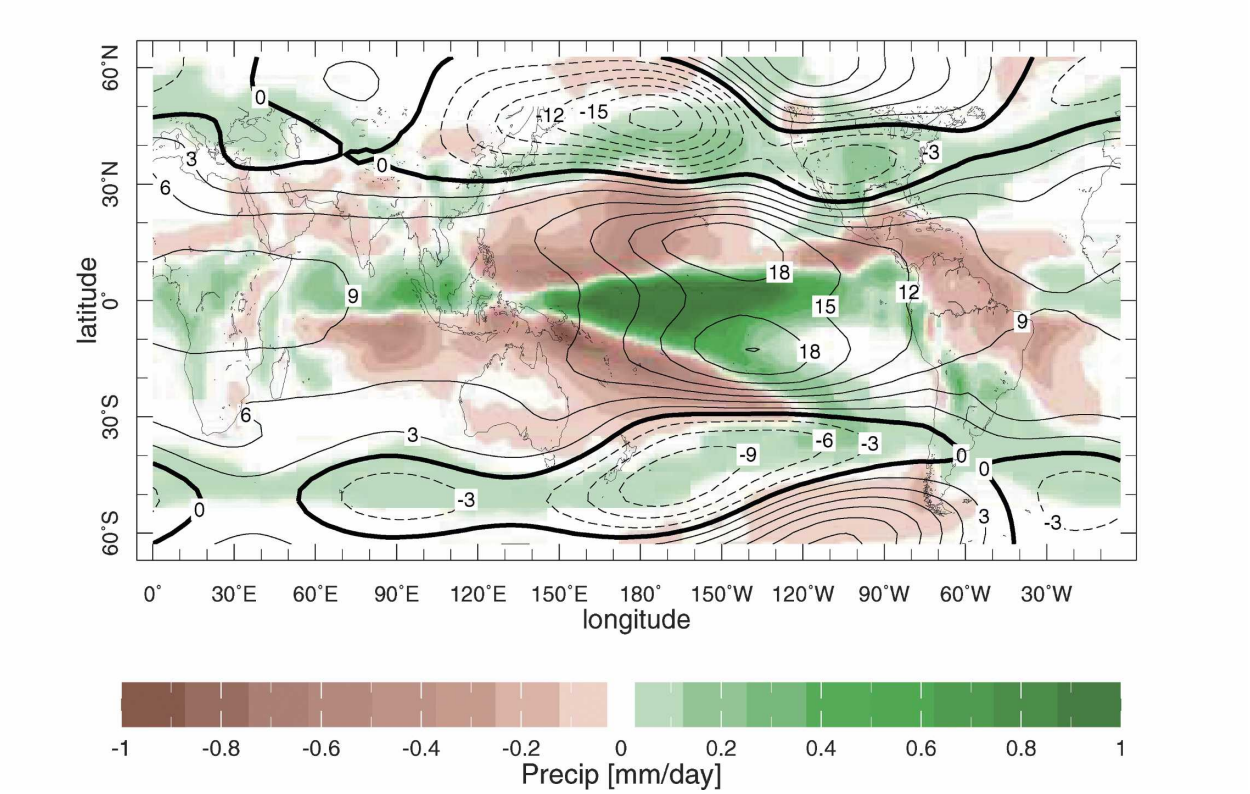

FIG. 6. The POGA-ML model ensemble mean 200-mb geopotential height (contours) and precipitation (colors) regressed onto a 6-yr low-pass-filtered time series of precipitation in the Great Plains for the period 1856–2000. The model was forced with observed SSTs in the tropical Pacific only and computed the SSTs elsewhere.

quences. The GOGA and POGA-ML model ensemble means and observed precipitation anomalies for the period between 1932 and 1939 including all months, relative to the period from 1856 to 2000, are shown in Fig. 7. Also shown in Fig. 7 are the observed SST anomaly at the same time, which the GOGA ensemble saw, and the SST anomaly from the POGA-ML ensemble, which combines the observed SST anomalies in the tropical Pacific and computed anomalies elsewhere.

In nature, almost the entire United States had reduced precipitation during this time with the exception of the Northeast. The largest reductions in precipitation occurred in the Great Plains north of Texas. Here the precipitation reduction amounts to about 10%–20% of the mean. Precipitation anomalies of the same sign across most of the United States (with opposite sign anomalies over Canada and, sometimes, the Northwest) are typical of ENSO-forced interannual variability (see Fig. 1 of S05; Mo and Higgins 1998; Cayan et al. 1998) and are distinct from less homogeneous patterns associated with southwest monsoon variability (Higgins et al. 1999). The 1930s and 1950s droughts, and the 1990s pluvial (see below), appear as low-frequency versions of the ENSO-forced variability.

The GOGA and POGA-ML model ensemble means (Figs. 7b and 7c) reliably capture the reduction of precipitation over the Great Plains, albeit with reduced intensity. They both extend the drought too far south into Mexico. They also underestimate the severity of the drought across the northern part of the United States. They are realistic in making the Northwest and Northeast wet. Despite the obvious errors, the models do simulate the broad brush aspects of the Dust Bowl drought. Both models simulate more precipitation over ocean regions south and east of the United States.

The observed SST anomalies for the 1932–39 period (Fig. 7d) show weak La Niña conditions. Given that the POGA-ML ensemble, which is only forced in the tropical Pacific, captures the essence of the Dust Bowl drought, there is no escaping the conclusion that these modest SST anomalies were indeed responsible for forcing the changes in atmosphere circulation that gave rise to the Dust Bowl. On the other hand, the GOGA model ensemble mean produces a stronger drought

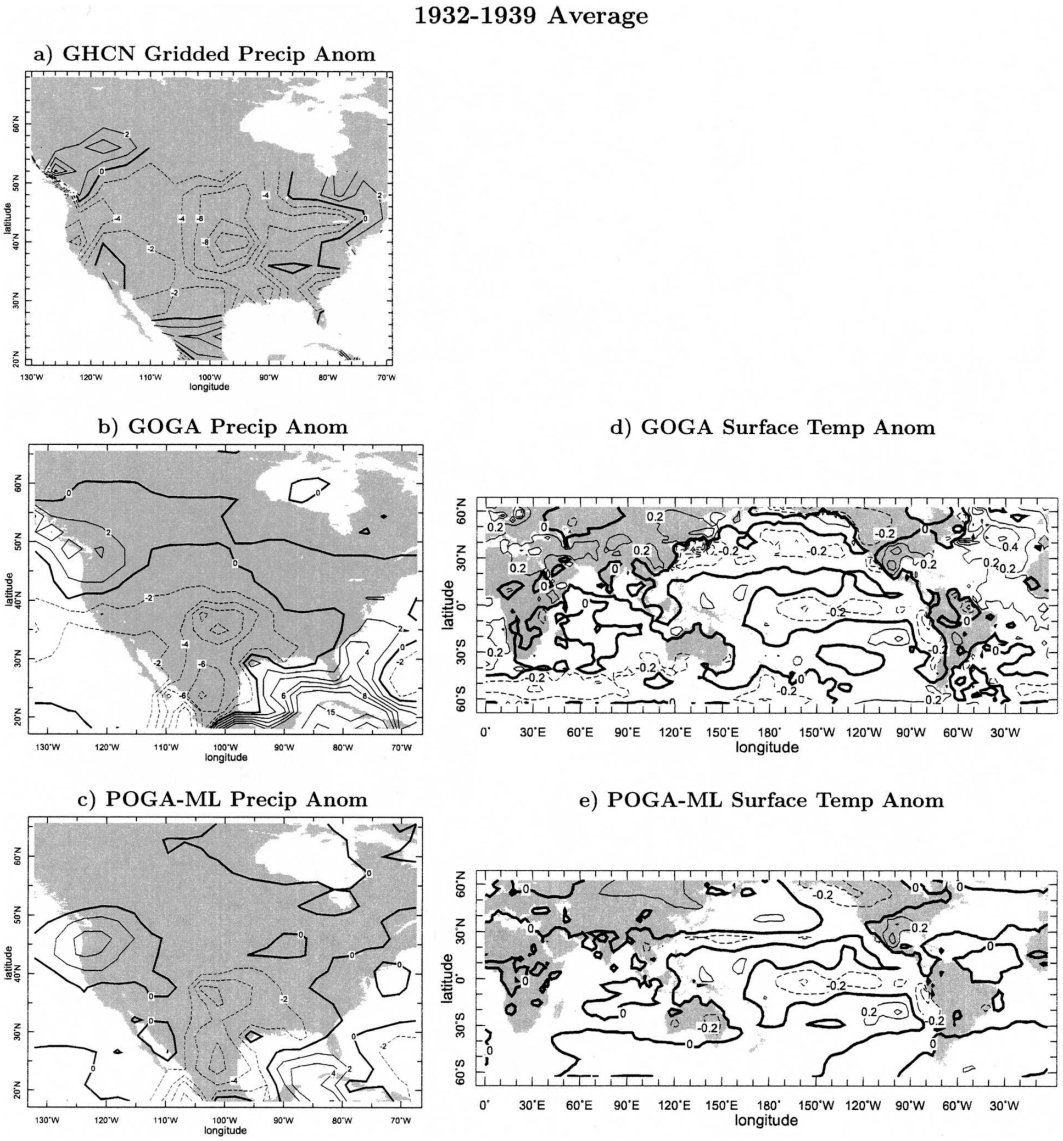

FIG. 7. Results for the 1932–39 Dust Bowl drought. (a) The observed precipitation anomaly for the 1932–39 period, (b) the precipitation anomaly from the GOGA ensemble, (c) the precipitation anomaly from the POGA-ML ensemble, (d) the observed SST anomaly, and (e) the SST anomaly from the POGA-ML ensemble. Precipitation units are mm month^{-1} and SST units are K.

than POGA-ML, and a larger increase of precipitation south and east of the United States, both of which may be because of the inclusion of SST forcing outside of the tropical Pacific. The POGA-ML ensemble produces SST anomalies typical of La Niña conditions: a warm midlatitude North Pacific Ocean, but with cool water along the Pacific coast of North America, and cool Indian and tropical Atlantic Oceans. The POGA-ML model also produces a modestly warm midlatitude North Atlantic Ocean. The real world was different in that, during the 1930s, the North Pacific Ocean was cool and the North Atlantic Ocean was warmer than modeled. It is possible that one, or both, of these regions of SST anomaly forced an atmosphere circulation anomaly that strengthened the drought. Examining another drought will help.

b. *The 1950s drought in the Southern Plains and Southwest*

From the late 1940s into the late 1950s, various areas of the Plains and Southwest experienced drought. The observed precipitation reduction between 1948 and 1957 is shown in Fig. 8a. In contrast to the 1930s, the 1950s drought did not effect the northern United States

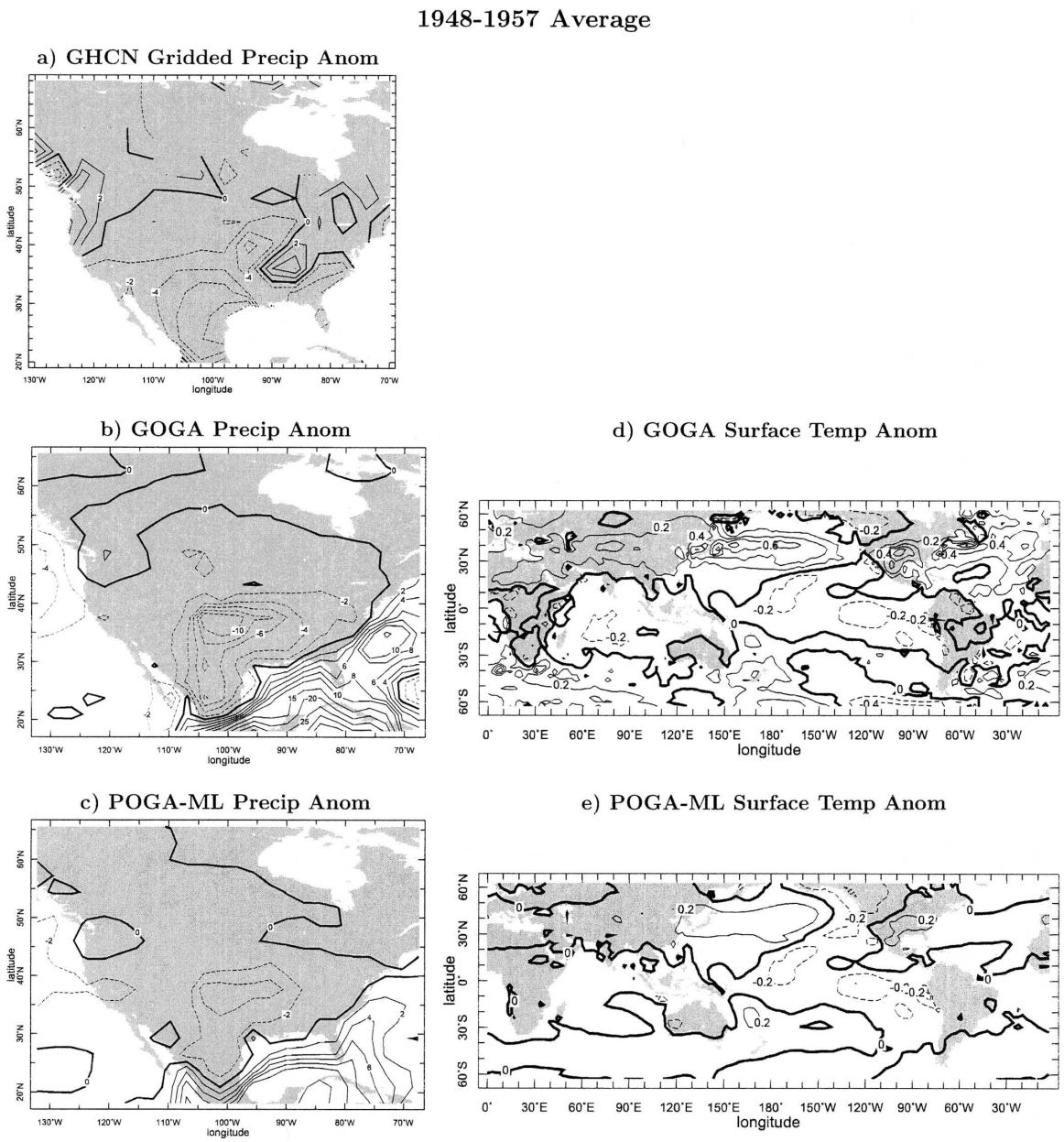

FIG. 8. Same as in Fig. 7, but for the 1948–57 drought.

and was instead focused on Texas, Oklahoma, New Mexico (where dust storms occurred), and northern Mexico. Maximum precipitation reductions were comparable to those in the 1930s. Both the GOGA and POGA-ML model ensemble means (Figs. 8b and 8c) produced droughts stretching from the southern Plains into northern Mexico but have the location of maximum precipitation reduction well north of that observed. The modeled pattern of drying is essentially the same as in the 1930s whereas there are obvious differences in location in the observations. Both model simulations show increased precipitation over the ocean south and west of the United States, with the GOGA anomalies being the largest, as for the 1930s.

As for the 1930s, the GOGA precipitation reduction exceeds that of the POGA-ML model. The global SST anomalies in the two models are shown in Figs. 8d and 8e. Both show classic La Niña patterns with a cool equatorial Pacific, cool Indian Ocean, and warm North Pacific. That the 1930s and 1950s modeled (and observed) droughts had obvious similarities, but the North Pacific SST anomalies were of opposite sign, sug-

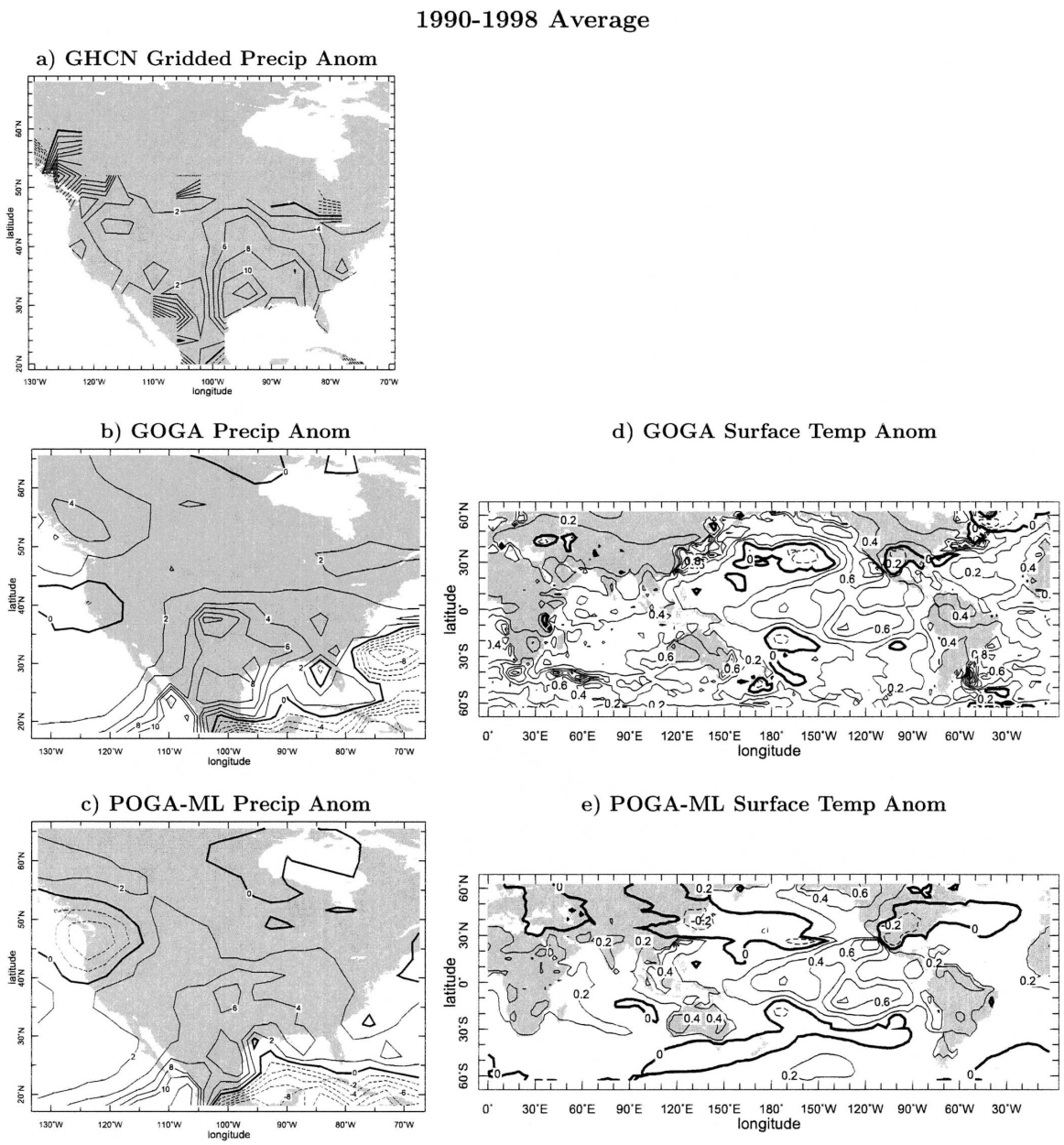

FIG. 9. Same as in Fig. 7, but for the 1990–98 pluvial.

gests that the atmosphere circulation anomalies responsible were primarily forced by the tropical SST anomalies, consistent with prior modeling studies (Lau and Nath 1994, 1996; Kushnir et al. 2002). As in the 1930s, the observed and modeled SST anomalies were warm in the North Atlantic. In all regions, the POGA-ML-modeled SST anomalies are too small.

c. *The 1990s North American pluvial*

Until the demise of the 1997/98 El Niño, the 1990s were a time of extraordinarily high levels of precipitation across most of the United States and northern Mexico. Figure 9a shows that no part of the States received less than climatological precipitation (as evaluated over 1856 to 2000). Precipitation was especially heavy in the Plains and the Mississippi Valley. As shown in Figs. 9b and 9c, the two models also make most of the United States and northern Mexico wet. Once more the GOGA model is more akin to nature than the POGA-ML model but still falls short of the observed precipitation anomaly. The models have reduced precipitation over oceans south (and east in GOGA) of North America.

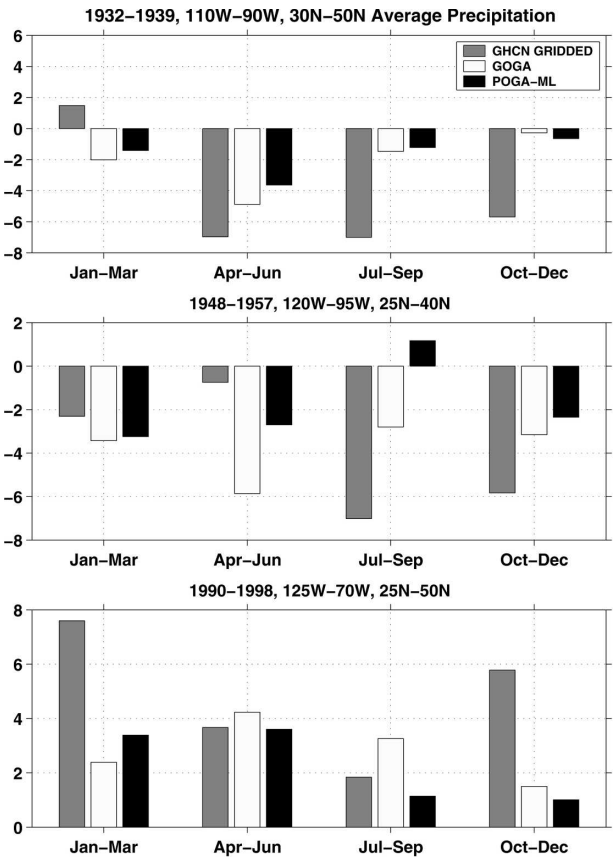

FIG. 10. Observed and modeled precipitation anomalies as a function of season for the periods 1932–39, 1948–57, and 1990–98. The left-hand bar is the observed anomaly, the middle bar is the GOGA-modeled anomaly, and the right-hand bar is the POGA-ML-modeled anomaly.

The observed SST anomaly is shown in Fig. 9d. Amidst the evidence of global warming is a classic El Niño–like pattern: the eastern and central equatorial Pacific were warm, the central North Pacific was cool, and warm waters lay offshore of the Pacific coast of North America. Much as La Niña–like conditions lead to reduced precipitation over North America, El Niño–like conditions lead to increased precipitation. The global SST anomalies in the POGA-ML ensemble appear more simply to be El Niño–like, lacking, as must be, the rather spatially uniform warming seen in observations.

d. Seasonality of the observed and modeled long-term precipitation variations

Figure 10 shows the precipitation departures from climatology as a function of season, that is, for example, by how much March–May precipitation averaged over 1932 to 1939 departed from the climatology for that season. The 1930s drought in the Plains was caused by a reduction in rain in the spring, summer, and fall seasons, while winters were actually slightly wetter than normal. During the 1950s drought in the Southwest, summer and fall were also very dry, but winter was also drier than normal. During the 1990s pluvial across North America, all seasons were wetter than usual but especially fall and winter.

The GOGA and POGA-ML models correctly simulate the spring drought in the 1930s but entirely fail to model the continued dry conditions in summer and fall. The inability of the models to reproduce the persistence from spring through fall of the precipitation reduction is the main reason why, averaged over the entire 1930s period, the modeled precipitation reduction is too small. The models correctly simulate the 1950s drought to have been caused by reduction of rain in winter as well as summer and fall but, incorrectly, also make spring dry. In the 1990s the models underestimate the wetness of the winter and fall but correctly make all seasons wetter than normal.

6. Atmospheric circulation anomalies during North American droughts and pluvials

The results presented so far have made clear that the modeled droughts and the 1990s pluvial were ultimately forced by SST variations in the tropical Pacific Ocean. In all three periods studied, there are significant precipitation anomalies in the summer half season. Summer precipitation anomalies over western North America could, conceivably, arise following winter anomalies, which have a well-established link to ENSO, with soil moisture providing the memory between seasons (Koster et al. 2004), or through summertime teleconnections. Here we examine the atmospheric circulation anomalies during the winter and summer half seasons and look for links between tropical Pacific SST variations and precipitation over North America. In the interest of brevity, only the GOGA ensemble will be considered. In general, the extratropical circulation anomalies in the POGA-ML ensemble are muted versions of those in the GOGA ensemble.

In this section, we analyze changes in precipitation (P) minus evaporation (E), which equals both the vertically integrated atmospheric moisture convergence and the soil moisture tendency less drainage. This will allow an assessment of the roles of local recycling of moisture and atmospheric circulation anomalies in creating and sustaining the droughts and pluvials. For brevity, we only show results for the 1930s (which were similar to the 1950s) and 1990s.

a. The 1930s Dust Bowl drought

Figures 11 and 12 show results from the GOGA simulations for the winters and summers, respectively, of the 1932–39 period. During the winter half year of the 1930s drought, $P - E$ was reduced, that is, atmospheric moisture divergence increased, over the southern United States and in large areas of the midlatitudes of each hemisphere (Fig. 11a), confirming that the persistent hydrologic variations retain the hemispherically and zonally symmetric character of the ENSO-related interannual variability.

Also, akin to ENSO variability, the Dust Bowl drought was associated with reduced $P - E$ in the central equatorial Pacific Ocean and an increase north of the equator associated with a northward shift of the intertropical convergence zone (ITCZ). The tropical Pacific $P - E$ anomalies closely track the SST anomalies (Figs. 11b and 12b), with cooler waters on the equator going along with less rain and warmer waters immediately north and south going along with more rain.

The modeled upper-tropospheric height anomalies in the 1930s are shown in Figs. 11a and 12a. There are wave trains extending from the area of reduced rain in the central Pacific and arching poleward and eastward into both hemispheres. These are particularly strong and well defined in the winter hemisphere and have the hallmarks of the Rossby wave propagation mechanism of tropical–extratropical teleconnections advanced by Hoskins and Karoly (1981). The height anomalies also display a zonally symmetric component with ridges overlying the midlatitude band of reduced precipitation.

The $P - E$ anomaly pattern during the summer half year of the 1930s is similar to the winter pattern except that the $P - E$ anomaly is slightly positive over the southern United States. That means that in that region the decrease in precipitation was actually exceeded by the decrease in local evaporation with increased atmospheric moisture convergence supplying the difference. This suggests that the negative $P - E$ anomaly from the winter half year, and reduced soil moisture, leads to reduced evaporation and precipitation the following summer. However there are also perturbations in the tropical Pacific atmosphere–ocean system and forced circulation anomalies during the summer season (Fig. 12b) that have the potential to effect global climate.

Comparing the 850-mb height anomalies (Figs. 11b and 12b) to the upper-tropospheric height anomalies, the circulation anomalies are seen to be largely barotropic. The one exception is over North America during summer: there is an anomalous high aloft and an anomalous low near the surface, a typical thermal low pattern. The anomalous low lies east of the center of the reduced summer precipitation. This is suggestive of a component of local forcing of the circulation in addition to the remote response to tropical forcing.

b. The 1990s pluvial

During the 1990s wet period, or pluvial, over North America (Figs. 13 and 14), the tropical Pacific was anomalously warm and there was increased $P - E$ over the equatorial Pacific Ocean and reduced $P - E$ to the immediate north. This provided for an anomalous forcing of atmospheric motions by diabatic heating that was the opposite of that in the 1930s and the 1950s. Consistently, there is now increased $P - E$ across the Northern Hemisphere midlatitudes.

The upper- and lower-tropospheric height anomalies are generally higher everywhere because the 1990s were, globally, the warmest decade in the 1856–2000 model simulation. Nonetheless the signature of Rossby wave propagation can still be discerned by noting that the height increase is lowest over the central North and South Pacific and over North America, while the heights are particularly high south of South America and over western Canada. The wave trains are essentially of opposite sign to those in the 1930s and 1950s. There is a surface high over the Gulf of Mexico during summer so, once more, the vertical structure is baroclinic here but barotropic elsewhere. The changes in $P - E$ were positive over most of North America except for the Pacific Northwest in winter and the Gulf Coast and Mexico in summer. These changes are opposite to those in the 1930s and 1950s.

c. The relationship between persistent precipitation and vertical velocity anomalies

Figures 11c through 14c show a close relationship between the anomalous vertical motion fields, the $P - E$ anomalies, and the low-level wind anomalies. During the simulated 1930s and 1950s droughts, there was anomalous descent across southern North America and the eastern Pacific Ocean, ascent over the western subtropical North America and the eastern Pacific Ocean, and ascent over the western subtropical North Atlantic Ocean. In the 1990s the pattern of anomalous vertical motion reversed. The patterns are such that locations of increased subsidence are locations of reduced precipitation. Reduced precipitation leads to reduced diabatic heating of the air column, which could induce anomalous subsidence. However, it is contended (S05) that it is the anomalous vertical motion that drives the anomalous precipitation.

The zonal mean component of the vertical motion is

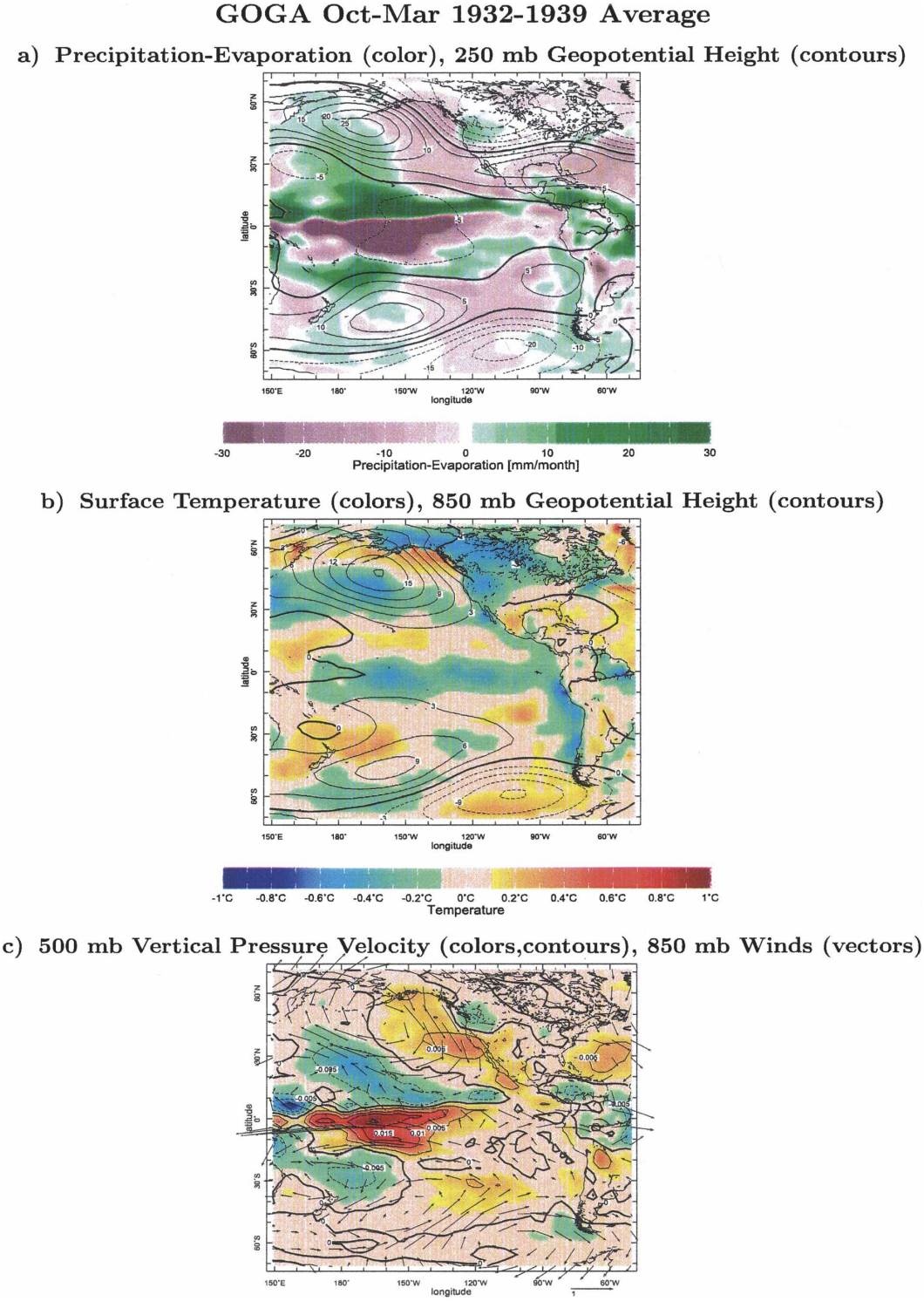

FIG. 11. Simulation of the winters (Oct–Mar) of the 1932–39 Dust Bowl drought with the GOGA model. (a) The precipitation minus evaporation and 250-mb height anomalies for the summers from 1932 to 1939, (b) the surface temperature and 850-mb height anomalies, and (c) the 500-mb vertical velocity and the 850-mb vector wind anomalies. Precipitation minus evaporation units are W m^{-2}, heights are in m, temperature is in K, and vertical velocity is in Pa s^{-1}.

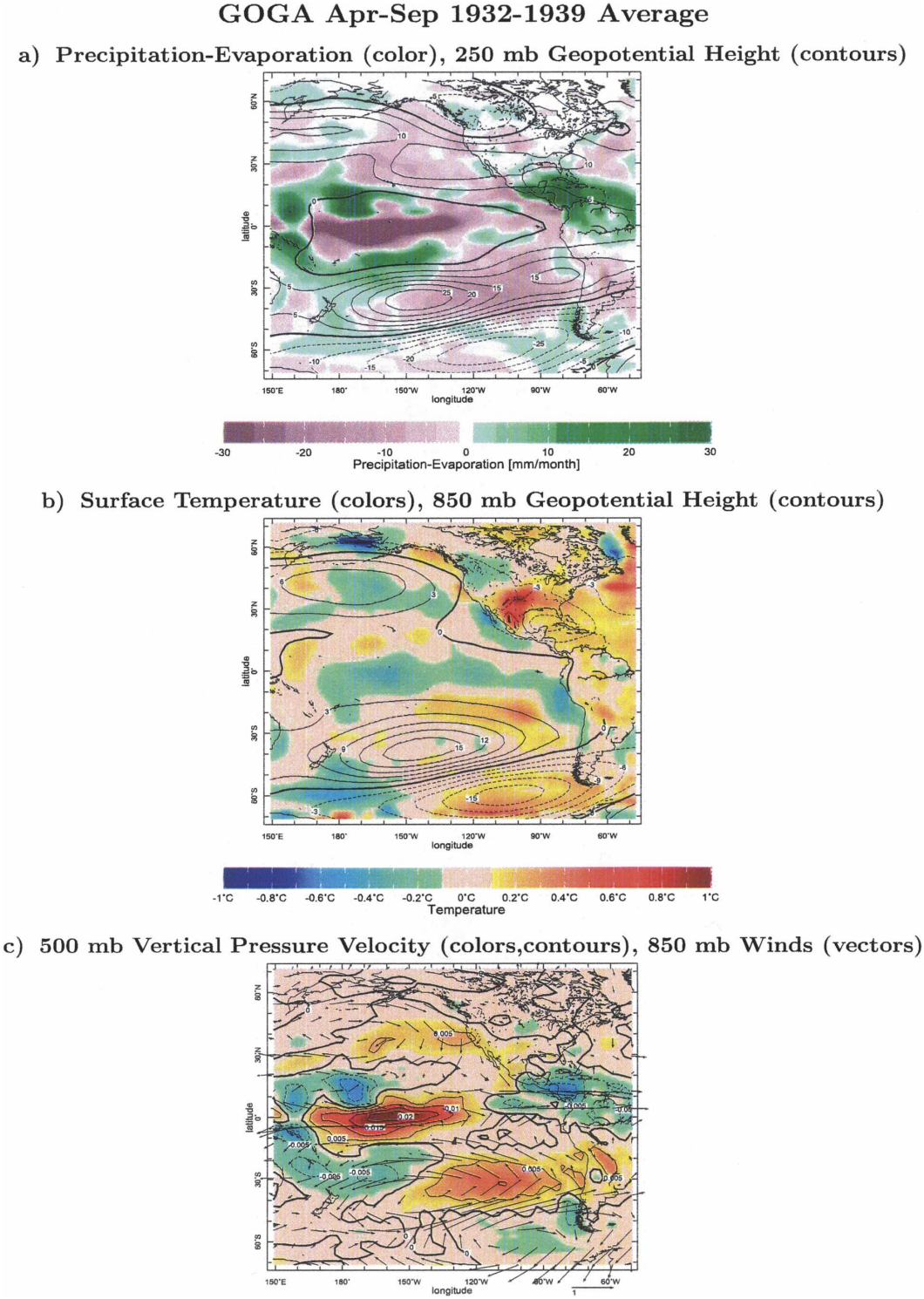

FIG. 12. Same as in Fig. 11, but for the summers (Apr–Sep) of the 1932–39 drought.

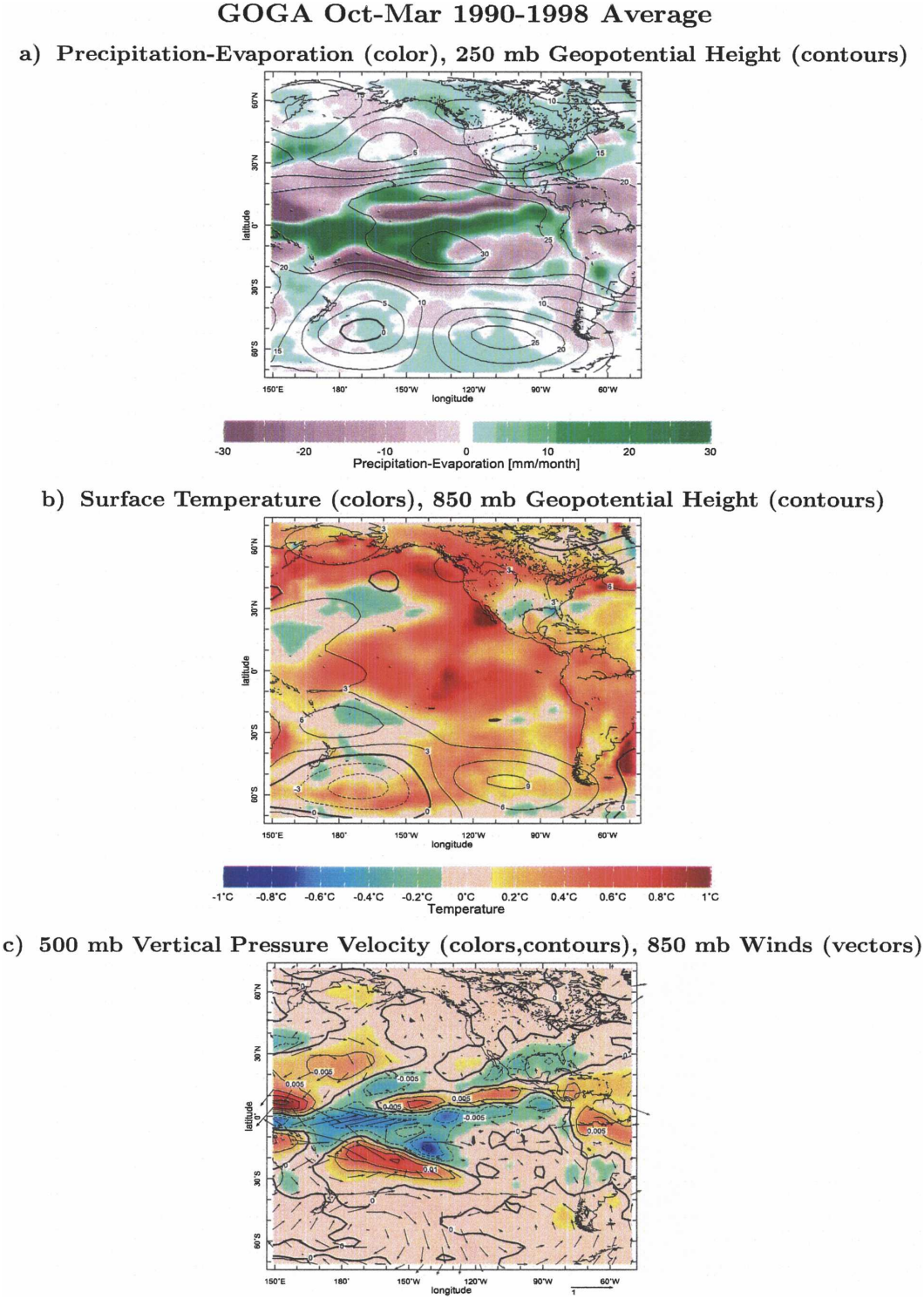

FIG. 13. Same as in Fig. 11, but for the GOGA simulation of the winters of the 1990–98 wet spell.

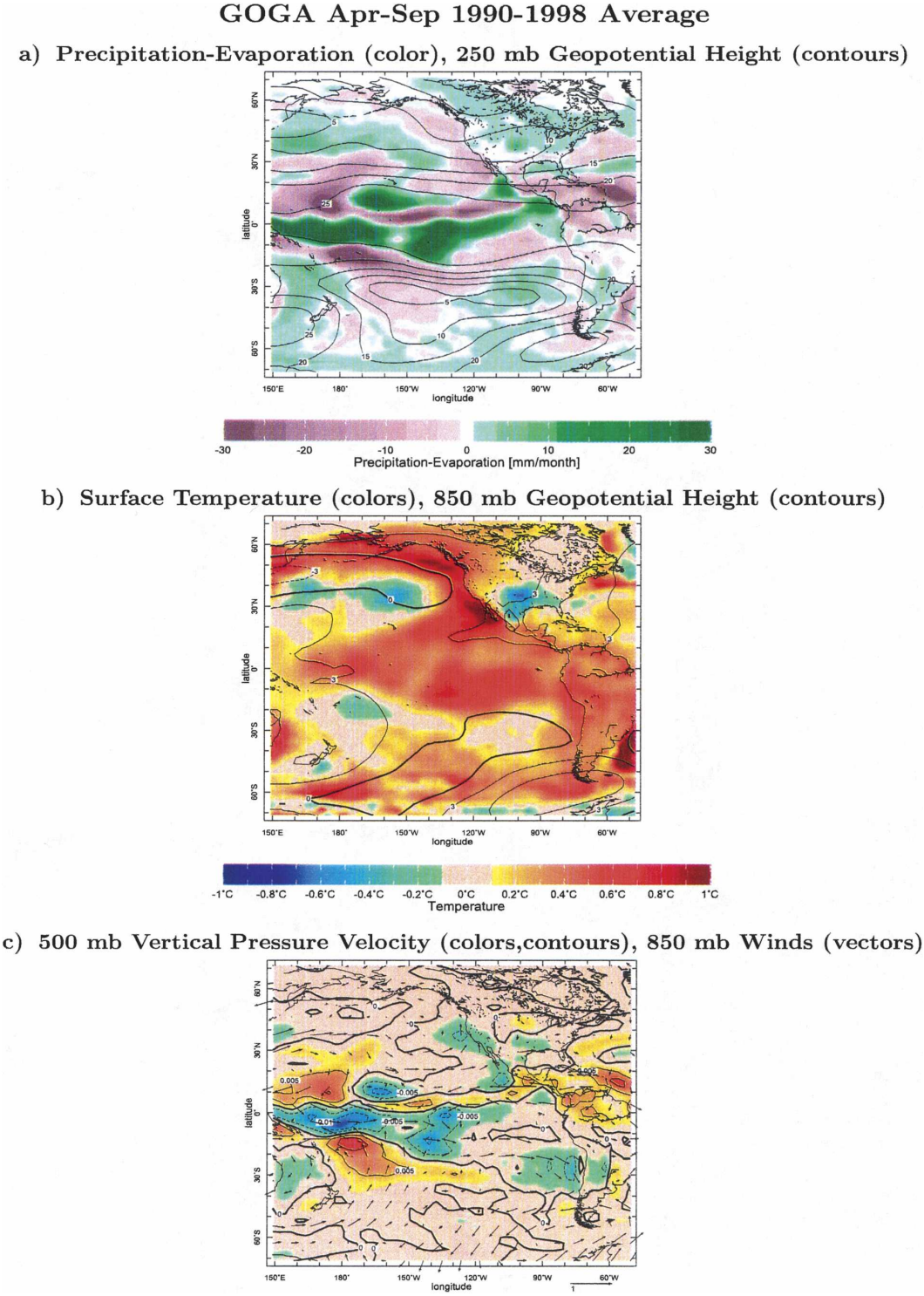

FIG. 14. Same as in Fig. 11, but for the GOGA simulation of the summers of the 1990–98 wet spell.

explained by interactions between the mean flow and transient eddies (S03; S05; and the next section), but regional patterns of anomalous vertical motion can have more complex causes. As shown in Figs. 11c–14c, regions of anomalous descent (e.g., the southern Plains and northern Mexico in the summer of the 1930s and 1950s) are regions of equatorward flow, and regions of anomalous ascent (e.g., southern North America in the summers of the 1990s) are regions of poleward flow. This is expected according to the basically Sverdrup balance between vortex stretching and advection of planetary vorticity that prevails in flow around the summer subtropical anticyclones (Rodwell and Hoskins 2001; Seager et al. 2003b).

7. The zonal mean context of the 1930s and 1950s droughts and 1990s pluvial

The decade-long precipitation anomalies in North America during the 1930s, 1950s, and 1990s were linked into near-global patterns of precipitation variations (Fig. 6). Here we analyze the zonally and hemispherically symmetric context of the persistent precipitation anomalies.

Figure 15 shows the change in zonal mean precipitation and evaporation for the April–October half year for 1932–39 within the GOGA ensemble (the 1950s drought was very similar in this regard and is not shown). There is reduced precipitation in the Northern and Southern Hemisphere midlatitudes. The northward movement of the ITCZ is also clear. The increased precipitation across the Northern Hemisphere midlatitudes in the 1990s also had its corollary in the Southern Hemisphere (Fig. 16). In each case, the zonal mean precipitation changes were not systematically related to changes in evaporation and instead required changes in atmospheric moisture transport.

Figures 15 and 16 also show the terms in the GOGA model's zonal mean atmospheric moisture convergence that balances $P - E$. These terms are the vertical mean convergence of moisture by the MMC, transient eddies, and stationary eddies. The convergence by the MMC is computed using the zonal mean specific humidity and meridional winds. The convergence by stationary eddies is computed using departures from the zonal mean of the specific humidity and meridional winds. The convergence by the transient eddies is computed using the departure from the monthly mean of daily values of the specific humidity and meridional winds.

S05 examined the observed and modeled zonal mean moisture budget variability associated with ENSO. The decadal variability examined here is very similar: the pattern of precipitation anomalies is best explained by

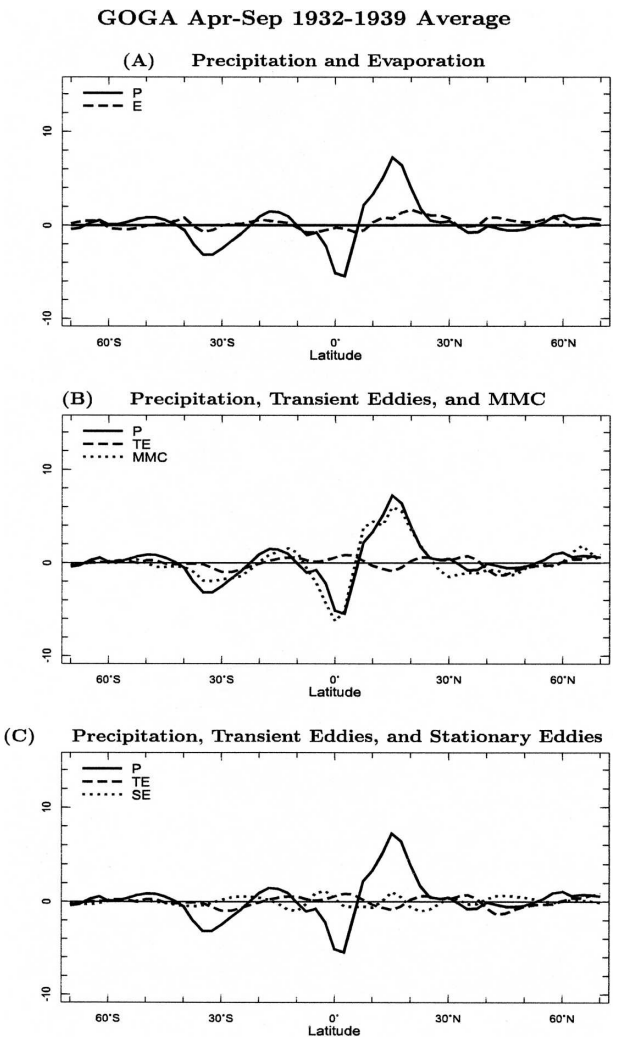

FIG. 15. Terms in the zonal mean moisture budget for the Apr–Sep half year over 1932–39. The precipitation is shown in all panels, but they also show (a) the evaporation, (b) the convergence of moisture by the MMC and transient eddies (TEs), and (c) the convergence of moisture by stationary eddies (SEs) and TEs. The convergences are vertically integrated over the atmospheric depth. All results are shown for the GOGA ensemble mean. Units are W m^{-2}.

the moisture convergence by the MMC. In the Tropics, this is explained by shifts in the ITCZ, northward during North American droughts and southward during the 1990s pluvial. In the midlatitudes, it is explained by the eddy-driven MMC, which has anomalous descent and low-level moisture divergence during dry periods and eddy-driven ascent during wet periods. Again, as for interannual variability, the zonal mean moisture convergences by the transient and stationary eddies largely cancel each other, an explanation for which is offered by S05.

The dynamical context of the hemispherically and

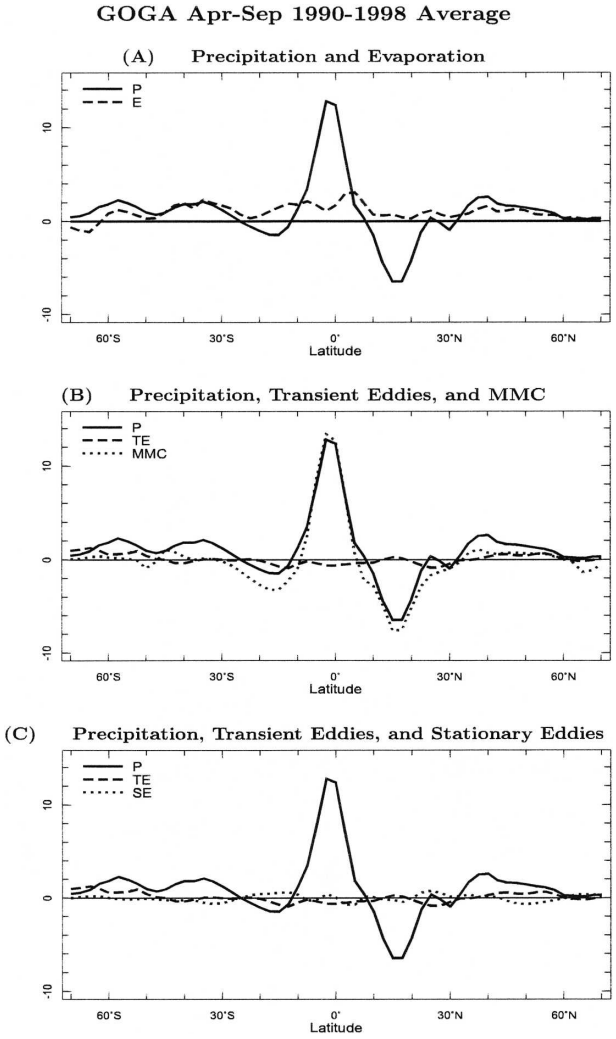

FIG. 16. Same as in Fig. 15, but for 1990–98.

zonally symmetric pattern in terms of the changes in zonal mean temperature and zonal winds is shown in Fig. 17 for the GOGA ensemble mean for the 1930s and 1950s droughts and the 1990s pluvial. During the droughts, the Tropics were cooler than normal, a consequence of the tropical SSTs. As a result, the subtropical jets were weaker. Following S03, the changes in the subtropical jets affect the propagation of transient eddies and the eddy-induced descent in midlatitudes that warmed the troposphere and suppressed precipitation. The zonal mean zonal winds strengthen on the poleward flank of the warm anomalies.

The dynamical changes in the 1990s are essentially the opposite (note the difference in color scale between this panel and the ones for the 1930s and 1950s). Amidst the global warming signal, the tropical troposphere warms the most, the subtropical jets strengthen, and the midlatitude troposphere remains relatively cool, a consequence of anomalous eddy-driven ascent. The zonal winds are weakened poleward of the weak midlatitude warming.

Just as for the observed interannual variability (S03), the changes in the jets affect the transient eddy momentum fluxes and the eddy-driven MMC. To illustrate this, Fig. 18 shows for the summer half year of the three periods the anomaly in transient eddy momentum flux, as simulated by the GOGA model. During the droughts, when the subtropical jets are weaker and more poleward, transient eddy momentum fluxes are anomalously negative in the northern tropical upper troposphere (S03) and positive in the northern midlatitudes. The meridional convergence of the eddy momentum flux, $-(1/a\cos^2\phi)\partial(\langle\overline{u'v'}\rangle\cos^2\phi)/\partial\phi$, is negative in the northern subtropics and positive in the northern midlatitudes. It must be balanced by the other dominant terms in the extratropical zonal mean zonal momentum equation, the Coriolis torque, $-(f + \langle\overline{u}\rangle\sin\phi/a\cos\phi)\langle\overline{v}\rangle$. Here angle brackets denote the zonal mean, overbars denote monthly means, primes denote departures from the monthly mean, ϕ is latitude, and other terms have their usual meaning.

As such, during droughts, the eddy momentum flux convergences induce poleward mean meridional flow in the subtropical upper troposphere and equatorward flow in midlatitudes, that is, upper-tropospheric convergence in the 30°–50° latitude range, forcing descent and suppressing precipitation. A similar sequence of events occurred in the Southern Hemisphere. An opposite set of adjustments occurred in the 1990s, in both the GOGA and the POGA-ML simulations. Anomalous transient eddy driving of the MMC is a fundamental mechanism whereby persistent tropical SST anomalies force persistent extratropical precipitation anomalies.

Just as these hemispherically symmetric patterns of persistent precipitation changes impacted North America, so did they impact South America. Drought was widespread in Uruguay in the 1950s (Pisciottano et al. 1994), while southern South America has been wet in the most recent decades (Barros et al. 2000). This is supported by analysis of the GHCN station data for the Americas for the 1930s, 1950s, and 1990s, which clearly shows precipitation changes arranged symmetrically about the equator (not shown).

8. Proposed mechanisms for generation of persistent midlatitude precipitation anomalies

Here we propose mechanisms whereby changes in tropical Pacific climate cause long-term droughts and pluvials over North America and in the midlatitudes in general. We will discuss the case of drought. The cycle

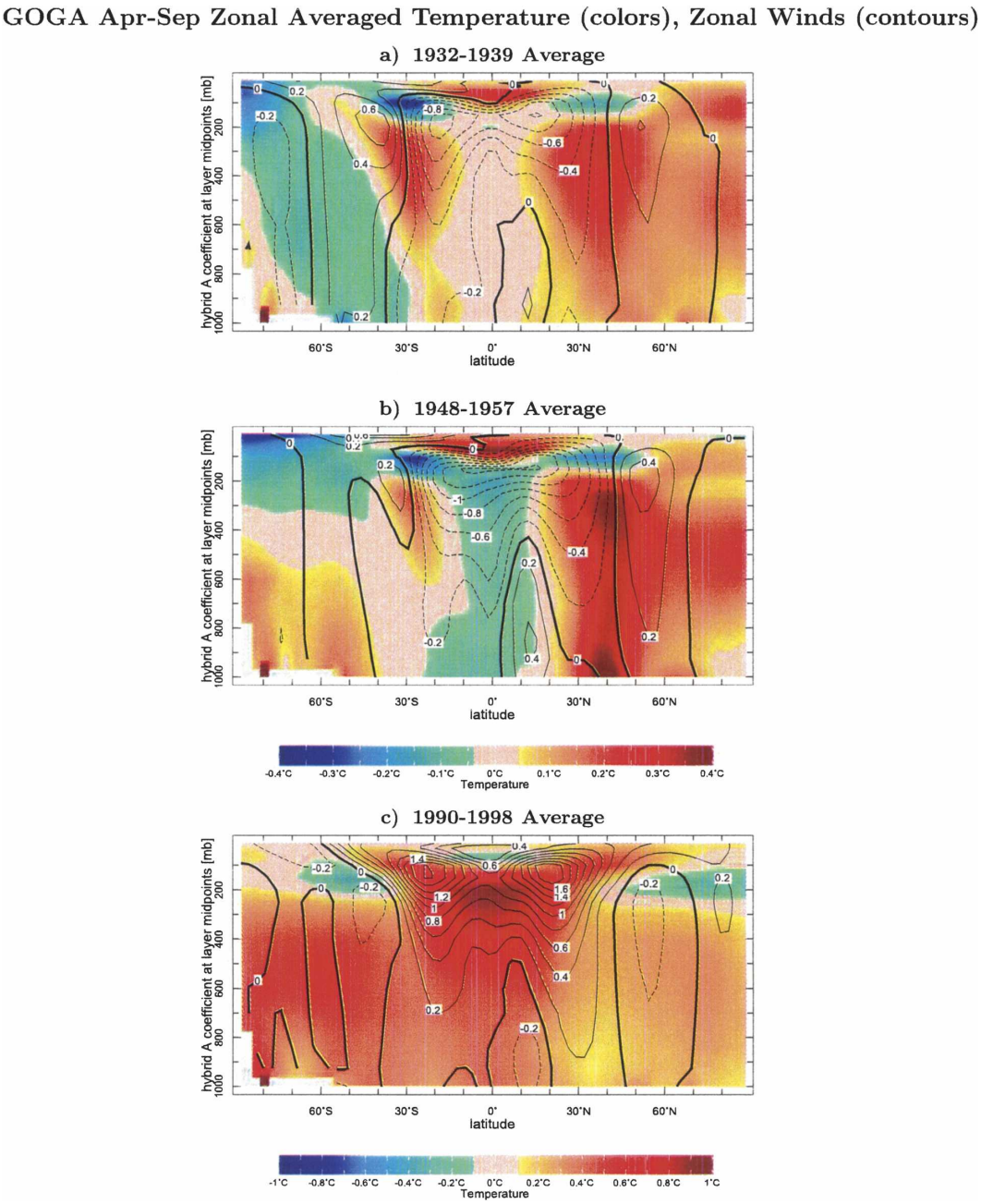

FIG. 17. The zonal mean zonal wind (contours; m s^{-1}) and zonal mean temperature (colors; K) for the Apr–Sep half year for the (a) 1932–39, (b) 1948–57, and (c) 1990–98 periods. All results are shown for the GOGA ensemble mean.

begins with cold conditions in the equatorial Pacific Ocean consistent with a persistent La Niña–like state and/or an absence of El Niños. The tropical Pacific Ocean is quite capable of generating such anomalies as part of its natural variability (Karspeck et al. 2004; Seager et al. 2004). Cold equatorial waters cause the tropical troposphere to cool and weaken the subtropical jets in both hemispheres. As such, transient eddies propagate less deeply into the tropical upper troposphere, creating there an anomalous equatorward eddy momentum flux that has to be balanced by the Coriolis torque operating on the mean meridional velocity. This causes poleward flow in the subtropical upper troposphere, convergence in the midlatitudes, high geopo-

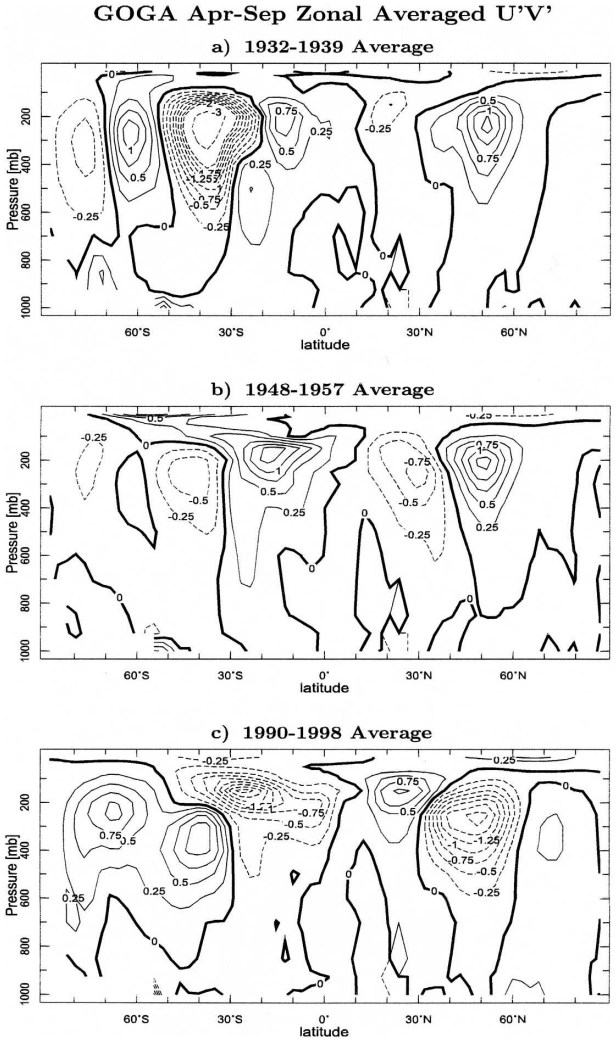

FIG. 18. The transient eddy momentum flux ($m^2 s^{-2}$) for the Apr–Sep half year of the (a) 1932–39, (b) 1948–57, and (c) 1990–98 periods. Results are for the GOGA ensemble mean.

tential heights, and subsidence into the lower troposphere. The subsidence both warms the midlatitude troposphere and suppresses precipitation. This explains the zonal mean signal.

The zonal symmetry is interrupted by Rossby wave propagation, into both hemispheres and in all seasons, forced by the shifts in the location of convection over the tropical Pacific Ocean. Previous studies (Trenberth and Branstator 1992) have shown that the wave train forced by the northward ITCZ displacement, caused by cold waters at the equator, intensifies the upper-level high over North America and the descent below. The anomalously dry regions of the midlatitudes are collocated with regions of anomalous descent with, we argue, the latter driving the former. In the lower troposphere, vortex compression associated with the descent is balanced by advection of planetary vorticity resulting in anomalous equatorward flow, obvious over the Plains in the 1930s and 1950s. This anomalous flow reduces the moisture inflow to North America from the Gulf of Mexico and could intensify the drought.

These circulation anomalies are fundamentally forced from the tropical Pacific, but the droughts are stronger when SST anomalies are imposed everywhere. It is suggested that once anomalous summertime descent has been set up over the Plains, the southerly flow on the western flank of the Atlantic subtropical anticyclone occurs farther east, over the eastern seaboard and western North Atlantic Ocean. The advection of warm, moist air poleward warms the ocean, assisting the development of precipitation in this region (Seager et al. 2003b) and leaving the continental region farther west drier than normal. This contention is supported by the warm waters and large increase in precipitation over the Atlantic Ocean south and east of the United States that occurs in the GOGA model when the Plains and Southwest are dry, a situation the POGA-ML also simulates, albeit at reduced strength, possibly because of model inadequacies in the surface fluxes or ocean mixed layer.

This suggested chain of events is offered as a testable hypothesis of how persistent droughts and pluvials are established over western North America, but only some links in the chain are supported by the results described here, or by other work. In particular, it is not possible to draw firm conclusions on the role of extratropical SSTs on the basis of experiments in which the SSTs are specified because this experimental design can interfere with the atmosphere–ocean interaction (Bretherton and Battisti 2000).

The current results suggest that the year-to-year persistence of the droughts, and the 1990s pluvial, was due to the year-to-year persistence of the tropical Pacific SST anomalies and that summer droughts can be forced by summer tropical SST anomalies. However, in agreement with prior studies (Schubert et al. 2004; Oglesby and Erickson 1989), a soil moisture feedback also appears to be important. In the model, summer precipitation reductions are associated with even larger evaporation reductions and follow strongly negative $P - E$ anomalies in the previous seasons that will have left the ground unusually dry.

9. Conclusions

We have presented results from model simulations of the long-term droughts over North America in the 1930s and 1950s and the prolonged wet period, or pluvial, in the 1990s and compared the simulations to observations. The main conclusions are as follows.

- The atmosphere GCM forced by the observed global SST anomalies from 1856 on simulates many aspects of the observed precipitation variations with periods of 6 yr or longer in the Plains and the Southwest. This indicates that a notable portion of the variations, including the droughts of the 1930s and 1950s and the pluvial of the 1990s were forced by global SST variations, confirming and extending earlier results (Schubert et al. 2004).
- Tropical Pacific SST variations are the ultimate driver of persistent droughts and pluvials over the Plains and Southwest, as evidenced by the ability of the model to reproduce these when only the tropical Pacific SST anomalies are specified. However there are notable, if unsystematic, differences between modeled and observed precipitation variations. These could be caused by natural variability, model error in the representation of tropical Pacific forcing of precipitation and SST variations outside the tropical Pacific, or model error in representing the impact of SST anomalies outside the tropical Pacific.
- There is a zonally and hemispherically symmetric component to the persistent droughts and pluvials, which argues for the tropical origin of the persistent precipitation regimes. During droughts, when the tropical Pacific is cool, the subtropical jets shift poleward and affect the momentum transports by transient eddies, resulting in eddy driving of descent in the midlatitudes of each hemisphere and suppressed precipitation.
- The hemispherically and zonally symmetric mechanism of tropical driving of precipitation variations works year-round setting up descent in midlatitudes during droughts. In addition, Rossby wave propagation from an ITCZ shifted northward by cool waters in the equatorial Pacific locally amplifies this signal over North America.
- Although tropically driven circulation anomalies are important during summer, over western North America during the droughts summer land surface evaporation is reduced by even more than the precipitation. This indicates an important role for soil moisture reduction in extending the droughts from winter and spring through to summer.
- Although the results presented only allow a tentative conclusion, once descent is established over North America, northerly low-level flow is required for vorticity balance, which reduces the intrusion of moist air from the Gulf of Mexico. This is a positive feedback on the drought. This also means that the southerly flow on the western flank of the subtropical anticyclone shifts east, warming the ocean offshore and allowing precipitation to establish itself there, which leaves the continental interior drier than usual.

The ultimate causes of persistent droughts and pluvials are persistent changes in tropical Pacific SSTs. These probably arise from the natural variability of the tropical Pacific climate system and may actually be predictable some years in advance (Karspeck et al. 2004; Seager et al. 2004). Furthermore, the tropical Pacific climate system is likely to respond to external, including anthropogenic, forcing by either becoming more El Niño–like or more La Niña–like. We do not know which, but either will have important implications for the future of precipitation over North America.

Acknowledgments. We wish to thank Walter Robinson and Ed Cook for many useful conversations. Three anonymous reviewers provided very useful critical reviews. This work was supported by NOAA Grants UCSIO-CU-02165401-SCF and NA16GP2024 and NSF Grants ATM-9986515 and ATM-9986072.

REFERENCES

Barros, V., M. E. Casteñeda, and M. Doyle, 2000: Recent precipitation trends in southern South America east of the Andes: An indication of climatic variability. *Southern Hemisphere Paleo- and Neoclimates,* P. P. Smolka and W. Volkheimer, Eds., Springer-Verlag, 187–206.

Bretherton, C. S., and D. S. Battisti, 2000: An interpretation of the results from atmospheric general circulation models forced by the time history of the observed sea surface temperature distribution. *Geophys. Res. Lett.,* **27,** 767–770.

Cayan, D., M. D. Dettinger, H. F. Diaz, and N. E. Graham, 1998: Decadal variability of precipitation over western North America. *J. Climate,* **11,** 3148–3166.

Cook, E. R., C. Woodhouse, C. M. Eakin, D. M. Meko, and D. W. Stahle, 2004: Long term aridity changes in the western United States. *Science,* **306,** 1015–1018.

Fritz, S. C., E. Ito, Z. Yu, K. R. Laird, and D. R. Engstrom, 2000: Hydrologic variation in the northern Great Plains during the last two millennia. *Quat. Res.,* **53,** 175–184.

Fye, F. K., D. W. Stahle, and E. R. Cook, 2003: Paleoclimatic analogs to twentieth-century moisture regimes across the United States. *Bull. Amer. Meteor. Soc.,* **84,** 901–909.

Hack, J. J., J. T. Kiehl, and J. W. Hurrell, 1998: The hydrologic and thermodynamic characteristics of the NCAR CCM3. *J. Climate,* **11,** 1179–1206.

Higgins, R. W., Y. Chen, and A. V. Douglas, 1999: Interannual variability of the North America warm season precipitation regime. *J. Climate,* **12,** 653–680.

Hoerling, M. P., and A. Kumar, 2003: The perfect ocean for drought. *Science,* **299,** 691–694.

Horel, J. D., and J. M. Wallace, 1981: Planetary-scale atmospheric phenomena associated with the Southern Oscillation. *Mon. Wea. Rev.,* **109,** 813–829.

Hoskins, B., and K. Karoly, 1981: The steady response of a spherical atmosphere to thermal and orographic forcing. *J. Atmos. Sci.,* **38,** 1179–1196.

Hurrell, J. W., J. J. Hack, B. A. Boville, D. L. Williamson, and

J. T. Kiehl, 1998: The dynamical simulation of the NCAR Community Climate Model Version 3 (CCM3). *J. Climate,* **11,** 1207–1236.

Kaplan, A., M. A. Cane, Y. Kushnir, A. C. Clement, M. B. Blumenthal, and B. Rajagopalan, 1998: Analyses of global sea surface temperature: 1856–1991. *J. Geophys. Res.,* **103,** 18 567–18 589.

Karspeck, A., R. Seager, and M. A. Cane, 2004: Predictability of tropical Pacific decadal variability in an intermediate model. *J. Climate,* **17,** 2842–2850.

Kiehl, J. T., J. J. Hack, G. B. Bonan, B. A. Bovile, D. L. Williamson, and P. J. Rasch, 1998: The National Center for Atmospheric Research Community Climate Model: CCM3. *J. Climate,* **11,** 1131–1149.

Koster, R., and Coauthors, 2004: Regions of strong coupling between soil moisture and precipitation. *Science,* **305,** 1138–1140.

Kushnir, Y., W. A. Robinson, I. Blade, N. M. J. Hall, S. Peng, and R. Sutton, 2002: Atmospheric GCM response to extratropical SST anomalies: Synthesis and evaluation. *J. Climate,* **15,** 2233–2256.

Laird, K. R., S. C. Fritz, K. A. Maasch, and B. F. Cummings, 1996: Greater drought intensity and frequency before AD 1200 in the northern Great Plains, USA. *Nature,* **384,** 552–555.

Lau, N.-C., and M. J. Nath, 1994: A modeling study of the relative roles of tropical and extratropical SST anomalies in the variability of the global atmosphere–ocean system. *J. Climate,* **7,** 1184–1207.

——, and ——, 1996: The role of the "atmospheric bridge" in linking tropical Pacific ENSO events to extratropical SST anomalies. *J. Climate,* **9,** 2036–2057.

Levitus, S. E., and T. Boyer, 1994: *Temperature.* Vol. 4, *World Ocean Atlas 1994,* NOAA Atlas NESDIS 4, 117 pp.

Mo, K. C., and R. W. Higgins, 1998: Tropical convection and precipitation regimes in the western United States. *J. Climate,* **11,** 2404–2423.

Oglesby, R. J., and D. J. Erickson, 1989: Soil moisture and the persistence of North American drought. *J. Climate,* **2,** 1362–1380.

Pisciottano, G., A. Diaz, G. Cazes, and C. R. Mechoso, 1994: El Niño–Southern Oscillation impact on rainfall in Uruguay. *J. Climate,* **7,** 1286–1302.

Rayner, N., D. Parker, E. Horton, C. Folland, L. Alexander, D. Rowell, E. Kent, and A. Kaplan, 2003: Global analyses of sea surface temperature, sea ice, and night marine air temperature since the late nineteenth century. *J. Geophys. Res.,* **108,** 4407, doi:10.1029/2002JD002670.

Reisner, M., 1986: *Cadillac Desert: The American West and Its Disappearing Water.* Penguin Books, 582 pp.

Rodwell, M. J., and B. J. Hoskins, 2001: Subtropical anticyclones and summer monsoons. *J. Climate,* **14,** 3192–3211.

Russell, G. L., J. R. Miller, and L.-C. Tsang, 1985: Seasonal oceanic heat transports computed from an atmospheric model. *Dyn. Atmos. Oceans,* **9,** 253–271.

Schubert, S. D., M. J. Suarez, P. J. Region, R. D. Koster, and J. T. Bacmeister, 2004: Causes of long-term drought in the U.S. Great Plains. *J. Climate,* **17,** 485–503.

Seager, R., N. Harnik, Y. Kushnir, W. Robinson, and J. Miller, 2003a: Mechanisms of hemispherically symmetric climate variability. *J. Climate,* **16,** 2960–2978.

——, R. Murtugudde, N. Naik, A. Clement, N. Gordon, and J. Miller, 2003b: Air–sea interaction and the seasonal cycle of the subtropical anticyclones. *J. Climate,* **16,** 1948–1966.

——, A. Karspeck, M. Cane, Y. Kushnir, A. Giannini, A. Kaplan, B. Kerman, and J. Velez, 2004: Predicting Pacific decadal variability. *Earth Climate: The Ocean–Atmosphere Interaction,* C. Wang, S.-P. Xie, and J. A. Carton, Eds., Amer. Geophys. Union, 115–130.

——, N. Harnik, W. A. Robinson, Y. Kushnir, M. Ting, H. P. Huang, and J. Velez, 2005: Mechanisms of ENSO-forcing of hemispherically symmetric precipitation variability. *Quart. J. Roy. Meteor. Soc.,* **131,** 1501–1527.

Stahle, D. W., and M. K. Cleaveland, 1988: Texas drought history reconstructed and analyzed from 1698 to 1980. *J. Climate,* **1,** 59–74.

Stine, S., 1994: Extreme and persistent drought in California and Patagonia during mediaeval time. *Nature,* **369,** 546–549.

Sun, D.-Z., 2000: The heat sources and sinks of the 1986–87 El Niño. *J. Climate,* **13,** 3533–3550.

Swetnam, T. W., and J. L. Betancourt, 1998: Mesoscale disturbance and ecological response to decadal climate variability in the American southwest. *J. Climate,* **11,** 3128–3147.

Trenberth, K., and G. W. Branstator, 1992: Issues in establishing causes of the 1988 drought over North America. *J. Climate,* **5,** 159–172.

——, and C. J. Guillemot, 1996: Physical processes involved in the 1988 drought and 1993 floods in North America. *J. Climate,* **9,** 1288–1298.

Woodhouse, C. A., and J. T. Overpeck, 1998: 2000 years of drought variability in the central United States. *Bull. Amer. Meteor. Soc.,* **79,** 2693–2714.

Worster, D., 1979: *Dust Bowl: The Southern Plains in the 1930s.* Oxford University Press, 277 pp.

Yulaeva, E., and J. M. Wallace, 1994: The signature of ENSO in global temperature fields derived from the microwave sounding unit. *J. Climate,* **7,** 1719–1736.